BRL

AD

TECHNICAL REPORT ARBRL-TR-02044

A PREDICTIVE SCHEME FOR THE BLAST ENVIRONMENT OF ARMY WEAPONS PART I. DEVELOPMENT AND VALIDATION OF THE THEORY

Bruce Henriksen
Benjamin Cummings

February 1978

USA ARMAMENT RESEARCH AND DEVELOPMENT COMMAND
USA BALLISTIC RESEARCH LABORATORY
ABERDEEN PROVING GROUND, MARYLAND

UNCLASSIFIED

SECURITY CLASSIFICATION OF THIS PAGE *(When Data Entered)*

REPORT DOCUMENTATION PAGE		READ INSTRUCTIONS BEFORE COMPLETING FORM
1. REPORT NUMBER TECHNICAL REPORT ARBRL-TR-02044	2. GOVT ACCESSION NO.	3. RECIPIENT'S CATALOG NUMBER
4. TITLE *(and Subtitle)* A Predictive Scheme for the Blast Environment of Army Weapons Part I. Development and Validation of the Theory		5. TYPE OF REPORT & PERIOD COVERED 6. PERFORMING ORG. REPORT NUMBER
7. AUTHOR(*e*) Bruce Henriksen Benjamin Cummings		8. CONTRACT OR GRANT NUMBER(*s*)
9. PERFORMING ORGANIZATION NAME AND ADDRESS US Army Ballistic Research Laboratory (ATTN: DRDAR-BLB) Aberdeen Proving Ground, MD 21005		10. PROGRAM ELEMENT, PROJECT, TASK AREA & WORK UNIT NUMBERS 1W662618AH80
11. CONTROLLING OFFICE NAME AND ADDRESS US Army Armament Research & Development Command US Army Ballistic Research Laboratory (ATTN: DRDAR-BL) Aberdeen Proving Ground, MD 21005		12. REPORT DATE FEBRUARY 1978 13. NUMBER OF PAGES 101
14. MONITORING AGENCY NAME & ADDRESS*(if different from Controlling Office)*		15. SECURITY CLASS. *(of this report)* UNCLASSIFIED 15a. DECLASSIFICATION/DOWNGRADING SCHEDULE

16. DISTRIBUTION STATEMENT *(of this Report)*

Approved for public release; distribution unlimited.

17. DISTRIBUTION STATEMENT *(of the abstract entered in Block 20, if different from Report)*

18. SUPPLEMENTARY NOTES

19. KEY WORDS *(Continue on reverse side if necessary and identify by block number)*

Muzzle Blast
Blast Overpressure
Unified Theory of Explosions

20. ABSTRACT *(Continue on reverse side if necessary and identify by block number)*

This is the first of three reports investigating the muzzle blast fields from the firing of Army weapons. This report presents theory and validation obtained by comparing analysis and muzzle blast field data. This first report limits investigation to the forward hemisphere of the blast field. The theory generally follows the data within the experimental error. The advantages of the theory are: its independence of empirical constants: and, the ease with which the computations are performed. Versions of the theory exist on minicomputers and on programmable pocket calculators.

DD FORM 1 JAN 73 1473 EDITION OF 1 NOV 65 IS OBSOLETE

UNCLASSIFIED

SECURITY CLASSIFICATION OF THIS PAGE *(When Data Entered)*

A PREDICTIVE SCHEME FOR THE BLAST ENVIRONMENT OF ARMY WEAPONS

PREFACE

An Important Note to the Reader

This memorandum report is the first of three parts of an analysis which predicts the blast wave properties produced by US Army weapons. Experience and reflection have ultimately shown a better way to perform the analysis in this as in many other endeavors: Thus, a three part report.

The preliminary analysis in this report was designed to establish the validity of a computationally simple approach to the problem. Emphasis was placed on elucidation of the theories with minimal comparison to data. Further work, to be presented in Part II, has applied the theory to a wide range of calibers. These extensions "clean up" some areas which have not previously been founded in rigorous analyses.

This new theory has not been completely exploited; e.g., work is in progress to apply the theory for prediction of the rearward blast field produced by recoilless rifles. This work will appear as Part III.

The analysis was initiated as a result of the promulgation of MIL-STD-1474A(MI), "Noise Limits for Army Materiel". Where previous standards had provided no serious constraints on the number of training rounds that could be fired by crews serving artillery pieces, the new standard introduced requirements which might make major changes in training schedules -- and costs. In particular, the section on impulse noise for personnel - occupied areas limit "blast" exposures ranging from 1000 to no exposures per day.

The potential cost of the experimental program to certify that all service locations for crew served weapons became a matter of concern to the Director of AMSAA. In turn, he suggested that experimental work could be minimized if the BRL produced an *a priori* predictive theory to guide such blast level experiments as would be necessary to implement the new Mil - Standard. Specifically, it was suggested that BRL Report 1019 had experimental data that could provide guidance in formulating a theory. In addition, the smaller computational scheme was to be preferred over hydro-codes since only scalar features of the flow field are involved in determination of compliance with the Mil-Standard.

To the individual who feels our approach is a fortuitous process, we offer the defense of H. Bethe: "If this is not the correct theory, it is still an excellent way to correlate the data".

This report presents our application of existing technology to the problem. We are indebted to our colleagues in BRL, AMSAA, and HEL for their cooperation, both in providing data and for the counsel and advice we received. Foremost, however, we are indebted to Francis Porzel, without whose theories this computational scheme would not have been possible.

TABLE OF CONTENTS

		Page
	PREFACE	3
	LIST OF ILLUSTRATIONS	7
I.	INTRODUCTION	9
II.	THEORY	11
	A. Interior Losses	14
	A.1 Energy Loss in the Presence of Boundary Layer Choke	15
	A.2 Energy Loss Due to Impedance to Flow by the Rough Wall	19
	B. The Unified Theory of Explosions	23
	B.1 The Generalized Equation of State	24
	B.2 The Mass Effect (MEZ) - The Mass Corrected Radius - Z	27
	B.3 The Waste Heat - Q	27
	B.4 The Form Factor	31
	B.5 The QZQ Hypothesis	32
	C. Peak Overpressure Calculation Scheme	35
	D. Aspherical Geometry	37
	E. Pulse Length Determination	40
III.	Comparison of Theory and Experiment	43
	A. Application of Spherical Explosion Theory to Muzzle Blast Overpressure Prediction	45
	A.1 The Moving Change Effect	45
	A.2 Revised Estimates for q	47
	A.3 Initial Cylindrical Shape	47

Page

B. Comparison of Theory and Experiment 52

B.1 Muzzle Blast Overpressure 52

B.2 Muzzle Blast Pulse Length. 54

C. Discussion 59

D. Summary and Conclusions 61

E. Suggested Future Studies - Areas not Considered in this Study 63

REFERENCES 65

APPENDIX. COMPUTATIONAL TOOLS 67

App-1 Code for the Texas Instruments SR-52 Pocket Calculator 68

App-2 Computer Code for the Theoretical Predictions 80

SYMBOL TABLE 88

DISTRIBUTION LIST 91

LIST OF ILLUSTRATIONS

Figure		Page
1	Pressure Volume Diagram for Adiobatic Expansion.	12
2	Division of Charge Mass	14
3	Boundary Layer Closure Due to Tube Roughness	15
4	Variation of Waste Heat with Pressure.	30
5	Cylindrical Charge Contribution to Transition. . . . . Radius Scaling	39
6	Data Adjustment for Muzzle Velocity Effect	48
7	Variation of Waste Heat with Distance.	49
8	Effect of Initial Charge Shape on Muzzle Blast . . . . . Overpressure	51
9	Muzzle Blast Overpressure M110E2 Self Propelled . . . . . Howitzer	53
10	Muzzle Blast Overpressure XM204 Towed Howitzer	55
11	Muzzle Blast Pulse Length M110E2 Self Propelled . . . . . Howitzer	56
12	Muzzle Blast Pulse Length M107 Artillery Gun	57
13	Muzzle Blast Peak Pressure M107 Artillery Gun	58
14	Linear Regression Fit to Muzzle Blast Peak Pressure- . . . . M107 Artillery Gun	60

INTRODUCTION

This report presents a method for predicting the muzzle blast overpressures and pressure pulse length emanating from guns during firing. The study was undertaken to determine if ear protection required for various guns, can be predicted *a priori*, i.e., without the necessity of heretofore required extensive experimentation. Our objective is to define a method which is independent of overpressure and pulse length data (i.e., no curve fitting) and which is simple and economical to use. The initial investigation is limited to large caliber guns without muzzle devices.

Previous investigations fall into two categories: (1) Large computer programs (the so-called hydrocodes) and (2) massive correlations of data. Representative examples of the first category include the works of Schmidt[1,2], Zoltani[3] and Ranlet[4]. These investigations provide insight into the basic physical processes but they require extensive computations to produce a solution. An excellent investigation within the second category is the work of Westline[5] which estimates the blast overpressure for various guns. His results include empirical constants which are necessary in describing the energy available to the blast from a specific gun. Neither the computational nor the empirical approach is acceptable in view of the objective--simple, general and economical predictive capability.

The most extensive work in blast overpressure prediction has been in the area of blast from explosions.[6] By this we mean that area in which spherical symmetry is obeyed. The technical literature of blast (explosions) abound with similarity parameters, scaling laws, governing

---

[1] *E.M. Schmidt, R.E. Shear, "The Flow Field About the Muzzle of an M16 Rifle," BRL Report No. 1692, Jan., 1974* (AD #916646L)

[2] *E.M. Schmidt, R.E. Shear, "Launch Dynamics of a Single Flachette Round," BRL Report No. 1810, Aug., 1975.* (AD #B006781L)

[3] *C.K. Zoultani, "Evaluation of the Computer Codes BLAST, DORF, HELP and HEMP for Suitability of Underexpanded Jet Flow Calculations," BRL Report No. 1659, Aug., 1973 (AD768708).*

[4] *J. Ranlet, J. Erdos, "Muzzle Blast Flow Field Calculations," BRL Contract Report No. 297, Apr., 1976.* (AD #B011967L)

[5] *P.S. Westine, J.C. Hokanson, "Prediction of Stand-off Distances to Prevent Loss of Hearing from Muzzle Blast," Rock Island Arsenal Report No. R-CR-75-003, Feb., 1975 (AD/A-005274).*

[6] *W.E. Baker, "Explosions in Air," University of Texas Press, Austin and London, 1973.*

relations for weak and strong shock waves, etc. We have applied this extensive work to the gun blast-field problem. This was done because at locations far from the source of the explosion, i.e., in the weak shock regime, asymmetrical effects are washed out and the shock wave can be modeled as though it originated from a spherical source of finite radius.

The gun blast problem requires analyses in addition to spherical explosion theory. The first is an estimate for the equivalent explosive yield which is produced by the gases escaping through the muzzle. Using the propellant charge energy (reduced by the projectile energy) is not correct because there are losses in the interior of the gun (heating, recoil, boundary layer generation, etc.). The second analysis addresses the (highly directional) energy release from the gun; which is now more cylindrically than spherically shaped. Lastly, other theories do not admit determination of pulse length without recourse to the above mentioned correlation techniques. The principal contribution of this report is a general treatment of these areas.

Assuming that the above problems have been solved, we still require a theory for the spherical blast wave. Scaling laws provide no help in an *a priori* analysis. A similitude analysis is required and perhaps the most well known is that by Sir G.I. Taylor in 1950[7]. His analysis reduced the several governing differential equations to one which can be solved by numerical quadratures. Seeking an even simpler form (mathematically) we have selected the Unified Theory of Explosions (UTE) as advanced by F.B. Porzel[8]. UTE is a comprehensive theory for explosions which offers simple analytic expressions for predicting blast parameters. This theory has been applied to a variety of explosions, from thermonuclear to small HE charges, and found to be valid to within a few percent.

The following sections include: II. Interior losses; III. Theory; IV. Presentation of Data, Comparison between theory and experiment, areas not addressed by our analysis, and an Appendix describing a computer code listing and sample output.

---

[7] *G.I. Taylor, "The Formation of a Blast Wave by a Very Intense Explosion: I Theoretical Discussion," Proc. R. Soc. A., 201, 159-174, (1950).*

[8] *F.B. Porzel, "Introduction to a Unified Theory of Explosions (UTE)," NOLTR-72-209, Sept., 1972 (AD-758000).*

II. THEORY

Analysis of the muzzle blast must be preceded by analyses (or at least definition) of the processes that occur in the gun interior, at the muzzle and of those which contribute to the shock wave propagation. The interior processes include compression and expansion waves, boundary layer flows, complex chemical reactions, heat transfer from the fluid to solid, friction, etc. The muzzle flow field develops with many similarities to the processes of underexpanded nozzles. There is a complicated interaction between the fluid of the gun and the atmosphere with the formation of a so-called shock bottle and associated Mach disks. Eventually, at a distance from the muzzle the flow field becomes more regular, resembling a geometrically transformed version of the blast wave that would be generated by an explosion. Current physical understanding of spatial non-uniformity is that the greatest transport of any quantity is in the direction of the largest gradient; hence, as the asymmetrical wave propagates outward it should approach spherical symmetry.

We propose that the complicated muzzle blast phenomena may be modeled as if it were initiated by a spherical explosive charge..

Ear protection required by military regulations is given in terms of the peak pressure and duration of the shock wave; that is, in terms of the energy in the shock wave. Consequently, our analysis is an account of the way in which the initial propellant energy is partitioned; into heat, friction, internal energy, propellant and projectile kinetic energy, etc. Finally, it is an account of that energy available to the shock wave. As we shall show, it is sufficient in the muzzle blast problem to monitor the energy transport processes--we do not require a detailed knowledge of the flow.

The assumption of an equivalency between the muzzle blast and spherical explosions has an important consequence. With this assumption we are able to use all of the analyses which occurred during the early phases of the nuclear explosion era for the solution of the muzzle blast problem. An excellent exposition of many of the theories and experimental data can be found in Baker[6]. Curiously missing are the theories we shall use--those of F.B. Porzel. In the following sections we shall derive and demonstrate Porzel's theories and show how these analyses can be applied to the muzzle blast overpressure problem.*

An important, underlying notion must be addressed first - the division of energies for shock wave overpressure prediction. In the following sections we shall speak of prompt energy and waste heat. Prompt energy is that energy which is (promptly) available for driving

*Most of Porzel's work is available in institutional or corporate documents. But; since Porzel's work is neither available in archival journals nor included in surveys like that of Baker, the authors have chosen to include their derivation of Porzel's work here.

the shock wave. Any energy which is lost from the shock wave, by whatever means, is termed waste heat. We emphasize that the waste heat is not necessarily lost from the system; it simply is not available to the shock wave. This differentiation is important because in many instances one would be led to say that neglecting this energy or that energy will have severe consequences when predicting certain phenomena other than the shock wave. We are concerned with only the shock wave, its strength and duration. Any energy which does not support the wave is, for our purposes, wasted (or delayed)*.

Prompt energy includes the pressure volume work in an expansion process and the kinetic energy of ordered motion imparted to the gas during the expansion. All other energy is waste energy. We can study the waste heat graphically with the help of the P-v diagram for an adiabatic expansion process (Figure 1).

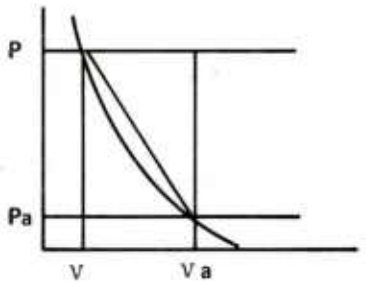

FIGURE 1

From the Rankine-Hugoniot relations[9], we find that the rectangle bounded by P = constant, v = constant and P = 0, v_a = constant is the total energy:

$$e_T = P\ (v_a - v).$$

The upper right triangle in the rectangle is the kinetic energy:

$$e_{KE} = \frac{1}{2}\ (P - P_a)(v_a - v).$$

The remaining trapazoidal area is the internal energy:

$$e_I = \frac{1}{2}\ (P + P_a)(v_a - v).$$

*Delayed energy is a subset of waste heat.

[9] *Y.B. Zel'dorvich, Yu P. Raizer, "Physics of Shock Waves and High-Temperature Hydrodynamic Phenomena," Academic Press, New York and London, 1966*

In an adiabatic expansion process (where real gas effects, such as ionization etc. are neglected) the gas pressure-volume will generally follow the curved line, the so-called Hugoniot or shock adiabat. The area between the adiabat and the straight line connecting Pv and $P_a v_a$ is the waste heat. At an infinite distance from the source of the blast all of the prompt energy has been converted to waste heat.

We can estimate the ratio of production of waste heat to the total energy using the Rankine-Hugoniot relations for changes across a shock wave:

$$\frac{e_I}{e_T} = \frac{\frac{1}{2}(P+P_a)(v_a-v)}{P(v_a-v)} = \frac{P+P_a}{2P} \quad .$$

For $P >> P_a$ the internal energy is approximately 1/2 the total, hence, half the energy is subject to waste (the kinetic energy is not subject to waste). In the acoustic approximation, $P \sim P_a$ and all the energy is wasted.

The following solution scheme is separated into two distinct analyses. The first is concerned entirely with the estimate for the prompt energy as the gases leave the muzzle. These calculations are used to predict a yield and radius for an equivalent spherical explosion which is treated as a separate problem.

A. INTERIOR LOSSES

Losses interior to the gun (keeping in mind the objective of finding values for waste heat and prompt energy) have been analyzed as:

(1) Kinetic energy given to the projectile and so lost to the supply of prompt energy; (2) other interior losses or delays of energy which amount to about 5/6's of the otherwise available energy*; (3) energy loss due to expansion; and, (4) energy loss due to tube roughness (in this case, rifling).

Item (1) is self evident. Item (2) is compatible with the mass effect (Section B-2) which states that initially the shock wave is driven by the mass of the explosive. If we view the propellant as a cube (Figure 2) we argue that only 1/6 of the mass is directed so as to be promptly available. The remaining mass which travels laterally and to the rear eventually exits the gun but because it is delayed, it does not directly contribute to the exiting shock wave.

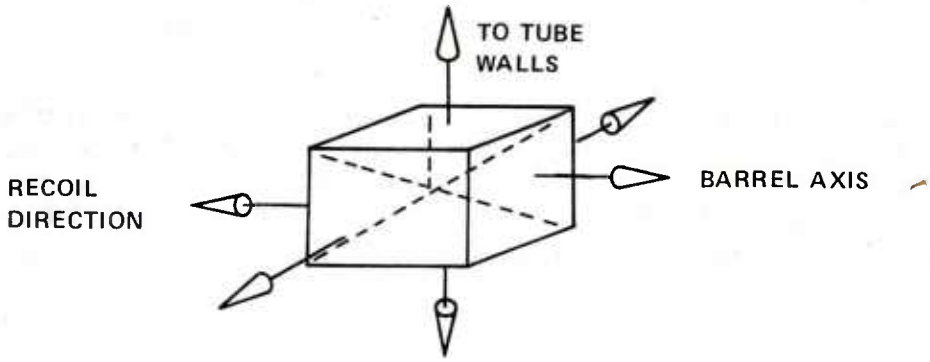

FIGURE 2

Regarding Item (3), we defined the prompt energy as including the kinetic energy of ordered motion. When a projectile travels down a barrel we expect a turbulent boundary layer (in which the ordered motion becomes random) to be formed.. After a sufficient length of the barrel has been traversed we further expect the boundary layer to close on itself; that is, at some distance behind the projectile there will be a point at which the turbulent motion extends across the entire diameter of the barrel. We treat the energy in the random motion as delayed and hence, wasted.

---

*This is consistent with Porzel's work applied to conical shock tubes.[10]

[10] *F.B. Porzel, "Correlation of Blast Simulators with a Unified Theory of Explosions," 3rd International Symposium on Military Application of Blast Simulators, Schwetzinger, Germany, Sept., 1972.*

Elementary flow theory tells us that when the velocity of a gas increases the static pressure decreases according to

$$P \propto K - aV^2$$

That is, given the same reservoir conditions (unchanged K), higher velocity gases have lower static pressures. The strength of the shock wave which is formed by the escaping gases will be determined by the static pressure at the projectile base (relative to an inertial reference frame). If we apply these notions to the material velocity (velocity of ordered motion) of the flow we can view the flow as proceeding from some stagnation pressure at the point of closure ($u_{material} \sim 0$) to some static pressure at the projectile base. This represents an energy reduction (via the pressure expansion) and is illustrated in Figure 3.

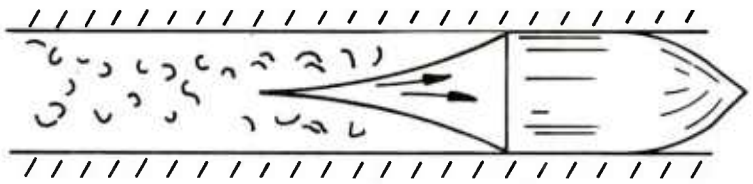

FIGURE 3

The last significant loss is due to the roughness (rifling) in the barrel. The energy in the fluid which interacts with (and is trapped by) the rough wall is delayed and is not available.

Item (1) is easily determined from the muzzle velocity and mass of the projectile. Item (2), which is not universally justifiable, is reasonable within the context of our energy definitions. The "proof of the puddin" is in the comparison with experiment (Section III). Following is the approach for determining the losses caused by effects (3) and (4). These analyses are obtained from Porzel[11].

A.1 Energy Loss in the Presence of Boundary Layer Choke

We are concerned with a loss of (stagnation) energy in the presence of a turbulent boundary layer in the gun barrel. The boundary layer, created by the moving projectile, grows as the projectile travels the length of the tube, but at some point the boundary layers created on the sides meet at the axis of the barrel. We shall speak of a closure of the boundary layer (Figure 3). Once this closure has occurred the energy of the gas is definitely separated into a region of ordered motion and a region where the significant portion of the energy is in the random motion of the fluid particles.

---

[11] *F.B. Porzel, "Study of Shock Impedance Effects in a Rough Walled Tunnel," Institute for Defense Analysis Research Paper P-330, Mar., 1969 (AD684790).*

Once closure has occurred we analyze the flow as a Bernoulli expansion from the stagnation pressure at the closure (the material velocity or ordered motion is essentially zero) to the static pressure at the base of the projectile. We associate the stagnation pressure with the maximum pressure and associate the pressure at the projectile base with the initial overpressure of the shock wave. To make the analysis tractable we assume there are no compression or expansion waves in the region from the closure point to the projectile (i.e., we can treat the expansion as adiabatic).

Our only interest is fluid motion along the axis of the barrel; hence, we can write the equation describing conservation of momentum in a moving coordinate system attached to the projectile as

$$\frac{\partial P}{\partial z} + \rho u \frac{\partial u}{\partial z} + \rho \frac{\partial u}{\partial t} = 0 \ , \qquad (1)$$

in which the material velocity is represented by u.

One may assume that once the boundary layer closure has occurred the distance from the closure point to the base of the projectile remains constant. That is, steady state prevails and $\partial u/\partial t \equiv 0$. (In Section III.A.1 we show that the ordered velocity is of the same order as the random speed in one direction.) Additionally, since the flow is adiabatic,

$$P = A\rho^{\gamma} \ . \qquad (2)$$

Substituting Equation (2) into (1), we obtain

$$(A/P)^{1/\gamma} \frac{dP}{dz} + u \frac{du}{dz} = 0 \ ,$$

which can be integrated to give

$$\frac{A^{1/\gamma}}{1-\frac{1}{\gamma}} P^{1-1/\gamma} + \frac{1}{2} u^2 = \text{constant} \ .$$

Since

$$\rho = \left(\frac{P}{A}\right)^{1/\gamma}$$

and, the speed of sound, a, is given by

$$a = \left(\frac{\gamma P}{\rho}\right)^{1/2}$$

we finally obtain

$$\left(\frac{2}{\gamma-1}\right) a^2 + u^2 = \text{constant.} \tag{3}$$

Equation (3) relates the material velocity and speed of sound at the closure point to the same quantities at the base of the projectile. This equation applies to the barrel reference frame provided the assumptions concerning constant closure-to-projectile-base distance and isentropic flow are not violated.

The constant in Equation (3) can be evaluated at the closure point where $u \ll 1$, $u \sim 0$. Thus Equation (3) becomes

$$\left(\frac{2}{\gamma-1}\right)a^2 + u^2 = \left(\frac{2}{\gamma-1}\right) a_c \quad , \tag{4}$$

where the subscript c denotes the choke point.

From Equation (4) we obtain

$$\left(\frac{a_c}{a}\right)^2 = 1 + \frac{\gamma-1}{2}\left(\frac{u}{a}\right)^2 \quad . \tag{5}$$

The adiabatic relation allows us to write

$$\left(\frac{a_c}{a}\right)^2 = \left(\frac{P_c}{P}\right)\left(\frac{\rho}{\rho_c}\right)$$

which can be reduced to

$$\left(\frac{a_c}{a}\right)^2 = \left(\frac{P_c/P_a}{P/P_a}\right)^{\frac{\gamma-1}{\gamma}} \quad . \tag{6}$$

Combining Equations (5) and (6) produce Equation (7):

$$\left(\frac{P_c/P_a}{P/P_a}\right)^{\frac{\gamma-1}{\gamma}} = 1 + \frac{\gamma-1}{2}\left(\frac{u}{a}\right)^2 \quad . \tag{7}$$

Let us assume, for the moment, that the length of the barrel is equal to the distance from the breech to the projectile base at the moment of boundary layer closure. The projectile would rapidly leave the driving gases because of the lateral expansion of these gases. The ordered motion is supersonic with respect to the ambient air hence a shock wave will form at the gas leading edge. At that instant we can use the Rankine-Hugoniot relations to determine the pressure ratio across this shock. (The shock wave which in fact produces the strongest overpressure). Specifically, we find[9]

$$\left(\frac{u}{a}\right)^2 = \frac{2(P_r-1)^2}{\gamma(\gamma-1)P_r\left(P_r + \frac{\gamma+1}{\gamma-1}\right)}, \quad P_r = P/P_a$$

and Equation (7) becomes

$$\left(\frac{P_{r_c}}{P_r}\right)^{\frac{\gamma-1}{\gamma}} = 1 + \frac{(P_r-1)^2}{\gamma P_r\left(P_r + \frac{\gamma+1}{\gamma-1}\right)}$$

or, denoting the pressure energy driving the shock wave by P_{r_s},

$$P_{r_c} = P_{r_s}\left[1 + \frac{\left(P_{r_s} - 1\right)^2}{\gamma P_{r_s}\left(P_{r_s} + \frac{\gamma+1}{\gamma-1}\right)}\right]^{\frac{\gamma}{\gamma-1}} \tag{8}$$

Equation (8) relates the reduction in the energy from the (essentially) initial pressure ratio, P_{r_c}, to the pressure ratio energy promptly available to the shock wave, P_{r_s}.

For current guns of interest, pressure ratios in excess of 100 are not unusual. Neglecting numbers of order unity (compared with 100) and using a specific heat ratio of 1.25 Equation (8) becomes, approximately,

$$P_{r_c} \sim (18.9)\ P_{r_s}$$

This means that the effect of the turbulent choke is a reduction in the available energy for driving the shock wave by a factor of approximately 19.

In order to estimate the point at which closure occurs we note that experimental results involving shock tubes with walls of known roughness give (denoting a roughness factor by H):

$$\frac{L}{D} = \frac{15}{H^{0.1}} \quad ; \tag{9}$$

as a very reasonable fit of the data[11]. The roughness factor is the ratio of the roughness height, h, to the unimpeded diameter of the tube.

A.2 Energy Loss Due to Impedance to the Flow by the Rough Wall

The prompt energy includes the ordered kinetic energy of the flow. Near the wall where the roughness of the wall can be felt by the flow, there is a local decrease in the kinetic energy as the flow encounters protuberances. These energy losses occur in addition to the boundary layer and we expect them to appear near the base of the projectile.

We shall assume that the change in the total energy is proportional to the kinetic energy (per unit volume), ϵ_{KE}, and the volume subtended by the average roughness of the barrel, which itself is a product of the roughness height, h, perimeter S and distance dL. That is

$$dE_T = -\alpha\ \epsilon_{KE} ShdL \tag{10}$$

where the constant of proportionality, α, can be viewed as an absorption coefficient.

It is reasonable to assume that the losses occur in a volume of dimensions A·D, where A is the cross-sectional area and D is the

diameter. If the total energy per unit volume is denoted by ε_T, then Equation (10) can be written

$$A \cdot D d\varepsilon_T = - \alpha \varepsilon_{KE} SH dL$$

or

$$d\varepsilon_T = - \alpha \varepsilon_{KE} \frac{S}{A} \frac{h}{D} dL \quad . \tag{11}$$

We can compare this relation with the classical exponential decay law by writing it in the form

$$\frac{d\varepsilon_T}{dL} = \left[- \alpha \frac{S}{A} \frac{h}{D} \right] \left[\frac{\varepsilon_{KE}}{\varepsilon_T} \right] \varepsilon_T \ .$$

That is,

$$\frac{d\varepsilon_T}{dL} \propto (\text{constant}) \cdot \text{fn}(P) \cdot \varepsilon_T$$

where the absorption coefficient is a pressure dependent function.

We can write Equation (11) in dimensionless form by setting the diameter, D, equal to the hydraulic diameter, i.e.,

$$D = \frac{4A}{S} \ ; \ \frac{S}{A} = \frac{4}{D} \ .$$

Equation (11) becomes

$$\frac{d\varepsilon_T}{\varepsilon_{KE}} = - 4 \alpha \frac{h}{D} d \left(\frac{L}{D} \right) \quad .$$

If we define

$$H \equiv \frac{h}{d} \ , \quad x \equiv \frac{L}{d}$$

we obtain

$$\frac{d\varepsilon_T}{\varepsilon_{KE}} = -4\,\alpha\,H\,dx \quad . \tag{12}$$

From the Rankine-Hugoniot relations, it is known that

$$\varepsilon_T = P\left(\frac{v_o}{v} - 1\right) ,$$

and

$$\frac{v_o}{v} = \frac{\mu P_r + 1}{P_r + \mu} \quad ; \quad P_r = P/P_a, \; \mu = \frac{\gamma+1}{\gamma-1}$$

hence,

$$\varepsilon_T = \frac{P_a P_r (P_r - 1)(\mu - 1)}{P_r + \mu} \quad .$$

The ratio of change of ε_T with the pressure ratio, P_r, is

$$d\varepsilon_T = \frac{(\mu-1)P_a(P_r^2 + 2\mu P_r - \mu)}{(P_r+\mu)^2}\, dP_r \quad . \tag{13}$$

Again, beginning with the Rankine-Hugoniot relations we can find that

$$\varepsilon_{KE} = \frac{(\mu-1)P_a(P_r-1)^2}{2(P_r+\mu)} \quad , \tag{14}$$

thus, the left hand side of Equation (12) is

$$\frac{d\varepsilon_T}{\varepsilon_{KE}} = 2\,\frac{(P_r^2 + 2\mu P_r - \mu)}{(P_r+\mu)(P_r-1)^2}\, dP_r \quad . \tag{15}$$

If we define

$$\Delta P_r = \frac{P-P_a}{P_a} = P_r - 1$$

and

$$\beta = \frac{2\gamma}{\gamma-1} = \mu+1$$

Equation (15) becomes

$$\frac{d\varepsilon_T}{\varepsilon_{KE}} = 2\,\frac{(\Delta P_r)^2 + 2\beta(\Delta P_r)+\beta}{(\Delta P_r)^2[(\Delta P_r)+\beta]}\,d(\Delta P_r). \qquad (16)$$

Combining Equations (16) and (12) the incremental energy loss due to the flow impedance is described by

$$\frac{(\Delta P_r)^2+2\beta(\Delta P_r)+\beta}{(\Delta P_r)^2(\Delta P_r+\beta)}\,d(\Delta P_r) = -2\,\alpha\,H\,dx \quad .$$

Integrating, we obtain

$$\frac{2\beta-1}{\beta}\ln(\Delta P_r) - \frac{\beta-1}{\beta}\ln(\Delta P_r+\beta) - \frac{1}{\Delta P_r} = \text{constant} - 2\,\alpha\,H\,dx \quad .$$

Denoting the left side by I, this relation determines the energy loss between two positions (1 & 2) down the barrel in the form

$$I_1 - I_2 = 2\,\alpha H\left(\frac{L_2-L_1}{D}\right). \qquad (17)$$

B. THE UNIFIED THEORY OF EXPLOSIONS - UTE

Next, we shall determine the shock wave properties by use of the Unified Theory of Explosions (UTE) as advanced by F.B. Porzel[8]. UTE is a comprehensive theory providing simple analytic expressions for blast parameter determination. UTE in total covers a gamut of conditions, geometries, etc.; however, we will examine only those parts pertinent to our problem. The concepts of prompt energy and waste heat were introduced in the beginning of this chapter. We now wish to show how this division of energies permits calculation of the overpressure for various ranges from the muzzle.

The prompt energy was defined as the kinetic energy of ordered motion plus the static overpressure energy. All other energy which does not directly support the wave was defined as waste heat. Hence, in general we can write

$$e_T = W + e_{KE} + Q \tag{18}$$

where W is the pressure volume energy, $W = \int P dv$, e_{KE} is the kinetic energy per unit mass (dynamic pressure) and Q is the waste heat.

The total prompt energy Y(R), the integral of the prompt energy, defined by

$$Y(R) = 4\pi \int_o^R (W + e_{KE})\, r^2 dr \tag{19}$$

is of particular interest. The boundary conditions for the shock expansion process are:

(1) At $R = R_o$, the initial charge radius, Y, is the hydrodynamic yield of the explosion, Y_o; and

(2) as R approaches infinity the shock wave must be completely dissipated hence $Y(\infty) \to 0$.

Substitution of Equation (18) into (19) gives

$$Y(R) = 4\pi \int_o^R (e_T - Q) r^2 dr = \frac{4}{3} \pi e_T R_o^3 - 4\pi \int_o^R Q r^2 dr \quad .$$

But boundary condition (2) requires that

$$\frac{4}{3}\pi e_T R_o^3 = 4\pi \int_o^\infty Qr^2 dr$$

hence,

$$Y(R) = 4\pi \int_R^\infty Qr^2 dr \ , \tag{20a}$$

from which the rate of loss of Y is found to be

$$\frac{dY}{dR} = -4\pi QR^2 \ . \tag{20b}$$

Specification of Q permits determination of the prompt energy and hence, of the static overpressure. The UTE becomes tractable if Q can be specified.

The abstraction which makes UTE tractable is the QZQ hypothesis which states:

$$QZ^q = \text{constant} \ . \tag{21}$$

where Z is a mass corrected radius. This relation permits Equation (20a) to be integrated in closed form yielding a simple analytic equation for the behavior of the prompt energy. Justification of this hypothesis requires development of an equation of state, determination of the mass corrected radius and the introduction of a form factor. The following sections develop the three concepts with the final section devoted to proof of the above relation (21).

B.1 The Generalized Equation of State - GES

Our analysis is designed to cover the spectrum of gaseous states from ambient to highly compressed. To do this, we require an equation of state capable of being extended into the dense gaseous state. The classical equation of state does not include interactions between particles caused by the long range force. It is derived by assuming spherical particles without an interaction potential.

Landau and Lifshitz[12] develop a correction term to the perfect gas law by assuming the gas is sufficiently dense that binary collisions are important but triple, quartic, etc., collisions may be neglected. Noting that the pressure can be found from the Gibbs free energy, F, by

$$P = - \frac{\partial F}{\partial v}$$

they find that, for binary collisions, the free energy is given by

$$F = F_p + N^2 \, K(T)/v$$

where N is the total number of particles, F_p is the free energy for the perfect gas state, v is the volume and $K(T)$ is proportional to the two particle interaction potential, U_{12}, via

$$K(T) \propto \int \left(e^{-U_{12}/kT} - 1 \right) dv$$

We can generalize* this result by writing

$$P = \Sigma \, \xi_i / v^{\eta_i}$$

where the ξ_i and η_i are constants embodying the interparticle interactions; these constants are determined from the thermodynamics of the processes. We can write this relation relative to the ambient pressure, P_a, as

$$P - P_a = \Sigma \left[\frac{\xi_i}{v^{\eta_i}} - \frac{\xi_i}{v_a^{\eta_i}} \right]$$

which may be reduced to

$$P - P_a = \Sigma \frac{\xi_i}{v_a^{\eta_i}} \left[\left(\frac{v_a}{v} \right)^{\eta_i} - 1 \right]$$

$$= \Sigma \frac{\xi_i}{v v_a^{\eta_i}} \left[\left(\frac{\rho}{\rho_a} \right)^{\eta_i} - 1 \right] . \qquad (22)$$

*Alternatively one can view the prior results as a specialization of Equation 22 (which follows).

[12] *L.D. Landau, E.M. Lifshitz, "Statistical Physics," Pergamon Press Ltd., London, 1958*

This is the Generalized Equation of State (GES) in the UTE used to calculate the waste heat.

Restricting our analyses to those regimes where real gas effects can be neglected, we have

$$P - P_a = \frac{\xi}{v_a^{\eta}} \left[\left(\frac{\rho}{\rho_a} \right)^{\eta} - 1 \right] .$$

One constant can be determined by recalling that $a_a^2 = (dp/d\rho)_a$, i.e.,

$$a_a^2 = \left(\eta \frac{\xi}{v_a^{\eta}} \rho^{\eta-1} / \rho_a^{\eta} \right) = \frac{\eta \xi}{v_a^{\eta} \rho_a}$$

These equations are combined to yield

$$P - P_a = \frac{\rho_a a_a^2}{\eta} \left[\left(\frac{\rho}{\rho_a} \right)^{\eta} - 1 \right] .$$

Use is made of two characteristics of a perfect gas (with constant ratio of specific heats), the adiabatic relation

$$P = (\text{constant}) \times \rho^{\gamma} \tag{23}$$

and

$$P_a = \frac{\rho_a a_a^2}{\gamma} ,$$

to obtain

$$P - P_a = \frac{\rho_a a_a^2}{\gamma} \left[\left(\frac{\rho}{\rho_a} \right)^{\gamma} - 1 \right] \tag{24}$$

and thus we conclude that on the average, $\eta = \gamma$.

B.2 The Mass Effect (MEZ) - The Mass Corrected Radius - Z

Blast energy is initially contained in the energetic material which produces the explosion, i.e., the propellant. Since no propellant burns instantaneously or (rarely) to completion, at initiation the shock wave is driven by the products of the reaction and by the as yet unburned particulate matter. As the shock wave expands and air is engulfed, some of the energy is transferred to the air and continues to drive the shock. Eventually, the shock wave leaves the residual mass because viscous drag on the particles reduces their speed relative to the shock speed. The effect is a reduction in the pressure since, as in the case of smoke which has a greater specific heat, the energy density in the residual mass is greater than that which would exist if only air were present.

In MEZ, the energy is assumed to be distributed between the particulate mass and air in direct proportion to their relative masses, that is,

$$\text{prompt energy} = (\text{prompt energy})_{air}\left[1 + \frac{BM}{\frac{4}{3}\pi R^3 \rho_a}\right] \tag{25}$$

where M is the particulate mass, B is the ratio of the mass prompt energy to that of air and $\frac{4}{3}\pi R^3 \rho_a$ is the mass of engulfed air at radius R. If we multiply the correction term by the cube of the radius we can define a new radius Z by

$$Z = (R^3+M')^{1/3} \tag{26}$$

where M' has a definition consistent with equation (25). We define Z to be the mass corrected radius.

B.3 The Waste Heat - Q

Our definition for the energy balance, Equation (18), permits us to write the waste heat equation as

$$Q = \Delta e_I - \int P dv \tag{27}$$

since the total energy reduced by the kinetic energy is the internal

energy. We can use Joule's Law[13] to write, for a perfect gas,

$$dE_I = C_v dT \ .$$

This equation, when coupled with the perfect gas law, allows us to write

$$\Delta e_I = \frac{\Delta Ei}{MASS} = \frac{Pv_I}{\gamma-1} - \frac{P_a v_a}{\gamma-1} \tag{28}$$

for the expansion process.

The pressure-volume energy is found using GES:

$$\int_{v_I}^{v_f} Pdv = \int_{v_I}^{v_f} \left\{ \frac{\rho_a a_a^2}{\gamma} \left[\left(\frac{v_a}{v} \right)^{\gamma} - 1 \right] + P_a \right\} dv$$

$$= \frac{\rho_a a_a^2}{(1-\gamma)\gamma} \left[\left(\frac{v_a}{v} \right)^{\gamma} v \right]_{v_I}^{v_f} + \left(P_a - \frac{\rho_a a_a^2}{\gamma} \right) (v_f - v_I) \ .$$

We assume that our expansion process is adiabatic, inviscid and non-conducting (i.e., isentropic). This is permissible since we are not concerned with the detailed structure of the shock wave. This assumption sets the second term zero since the assumption results in $P_a = \rho_a a_a^2/\gamma$. The first term is

$$\frac{\rho_a a_a^2}{(1-\gamma)\gamma} \left[\left(\frac{v_a}{v_f} \right)^{\gamma} v_f - \left(\frac{v_a}{v_I} \right)^{\gamma} v_I \right] .$$

If we associated the final state with v_a we can write the integral as (dropping the subscript I)

$$\frac{P_a v_a}{1-\gamma} \left[1 - \left(\frac{v_a}{v} \right)^{\gamma-1} \right] \ .$$

---

[13] *L.M. Milne-Thomson, "Theoretical Hydrodynamics," The Mac Millan Co., New York, 1950*

Again making use of the isentropic relation, Equation (23), we finally obtain the pressure-volume energy

$$W = \int P dv = \frac{Pv}{\gamma-1} \left[1 - \left(\frac{v}{v_a}\right)^{\gamma-1}\right]. \tag{29}$$

Combining Equations (27)-(29), we obtain a dimensionless waste heat, Q*:

$$Q^* = \frac{\rho_a Q}{P_a} = \frac{1}{\gamma-1}\left[\frac{\rho_a}{\rho}\left(\frac{P}{P_a}\right)^{1/\gamma} - 1\right] . \tag{30}$$

Lastly, we note that the density ratio, $\rho_a/\rho \equiv D$, is given in terms of the pressure by the Hugoniot relations as

$$D = \frac{\rho}{\rho_a} = \frac{\frac{\gamma+1}{\gamma-1} P_r + 1}{P_r + \frac{\gamma+1}{\gamma-1}} . \tag{31}$$

We are interested in the behavior of Q* with pressure. For small overpressures Equation (30) can be expanded by using the binomial theorem:

$$Q^* \cong \frac{\gamma+1}{12}\left(\frac{\Delta P_r}{\gamma}\right)^3 \tag{32}$$

for $\Delta P_r = (P - P_a)P_a << 1$. Equation (32) states that in the acoustic wave approximation the dimensionless waste heat varies as (approximately) P^3. For high overpressures (say $\Delta P_r > 10$) Q* is found to more approximately follow [8]

$$Q^* = 10^{\frac{(22-L)(L-1)}{16}}, \quad L = \mathrm{Log}_{10}(\Delta P_r) \tag{33}$$

and gives approximately a linear variation between Q* and ΔP_r. This is illustrated in Figure 4.

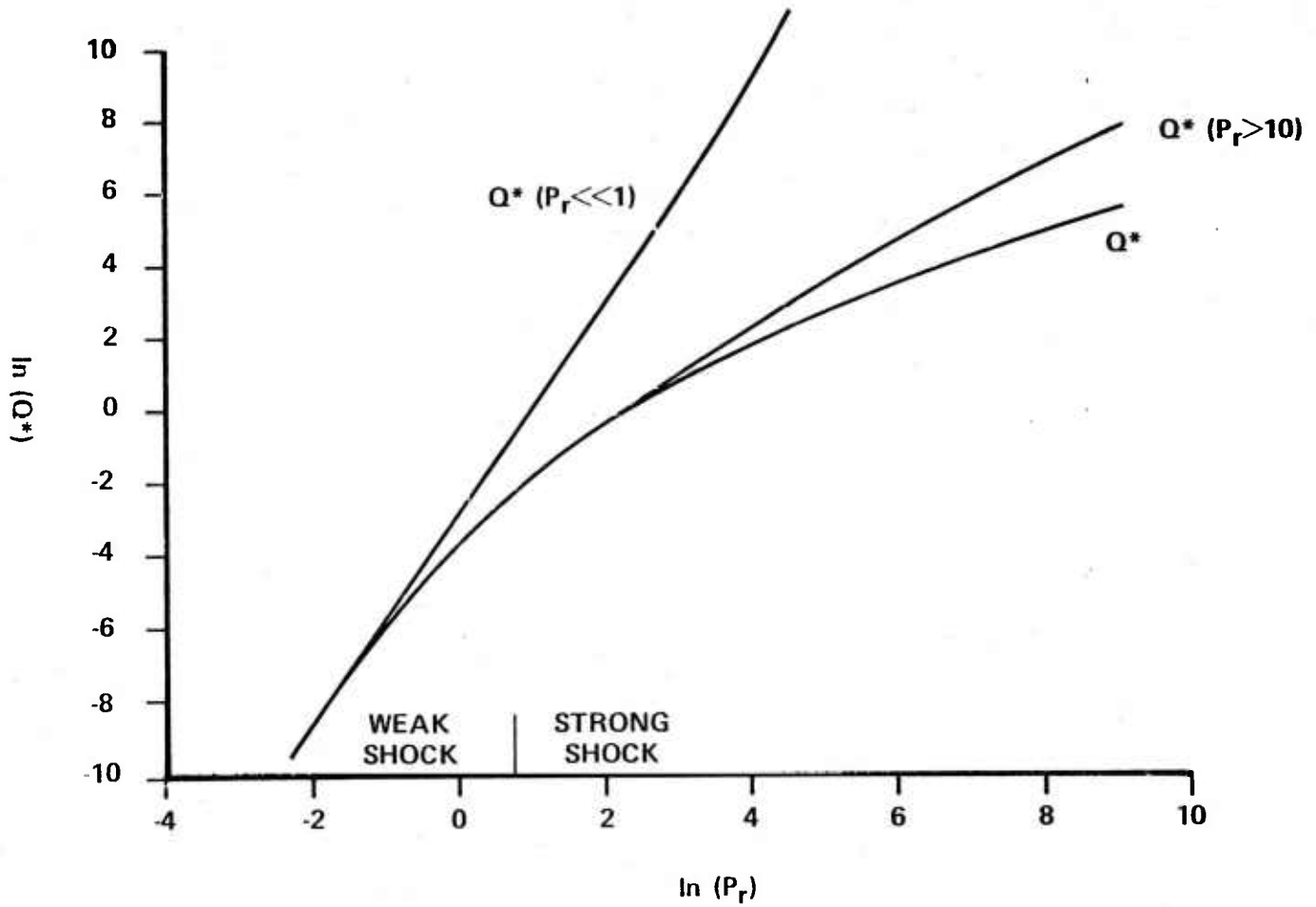

Figure 4. Variation of waste heat with pressure

B.4 The Form Factor

We introduce one more concept in order to justify the QZQ hypothesis: the form factor, F. To quote Porzel[8]: "Probably the most important single experimental fact learned about explosions in the past 30 years is the fact that they scale, and over enormous ranges of yield. This means there must exist a quantity F which is not unique to the explosion, requiring a separate calculation for each, but some average energy, a form factor common to all explosions. If we can determine it for one, we can determine it for all similar explosions."

In general, we can express the integrated prompt energy as

$$Y = 4\pi \int_0^R (W+K) r^2 dr \ ,$$

the terms of which can be arranged as follows:

$$Y = \frac{4}{3}\pi R^3 P \left\{ \frac{1}{P} \int_0^R 3(W+K) \left(\frac{r}{R}\right)^2 d(r/R) \right\}$$

or

$$Y = \frac{4}{3}\pi R^3 P \left\{ \frac{1}{P} \int_0^R (W+K) r^2 dr \div \left(P \int_0^R r^2 dr\right) \right\} \quad . \tag{34}$$

We denote the bracketed term by F, the form factor. It is a ratio of the average energy in the wave to the peak pressure. The integrated prompt energy can thus be written

$$Y = \frac{4}{3}\pi R^3 \cdot P \cdot F \tag{35}$$

Blast energy	=	shock volume	peak pressure at shock wave	average energy on interior rel. to peak pressure.

We wish to determine the dependence of the form factor on the radius. Since $Y \sim QR^3$ one may rewrite Equation (35) as

$$PF(P) \sim QR^3 / \left(\frac{4}{3}\pi R^3\right) \sim Q$$

In the strong shock regime $P \sim R^{-3}$ and since $Q \sim P \sim R^{-3}$, F is essentially constant. In the weak shock regime the spherical wave is very nearly planar and acoustic theory gives $P \sim R^{-1}$. But $Q \sim P^3$ in the weak shock regime hence $F \sim R^{-2}$.

We now have the tools necessary to justify the QZQ hypothesis.

B.5 The QZQ Hypothesis

The blast energy balance is

$$Y_o = 4\pi \int_0^R (W+K) r^2 dr + 4\pi \int_0^R Q r^2 dr.$$

Initial yield = prompt energy + waste heat.

Using the results of the previous section Y_o can be written

$$Y_o = \frac{4}{3}\pi R^3 PF + 4\pi \int_o^R Q r^2 dr \ .$$

Differentiation of Y_o with respect to R (noting the $1/4\pi\ d(Y_o)/dr = 0$) gives

$$QR^2 + R^2 PF + \frac{1}{3} R^3 \frac{d}{dR} (PF) = 0 \ .$$

Dividing these results by R^2 P F we have

$$\frac{Q}{PF} + 1 + \frac{1}{3} \frac{1}{RPF} \frac{d}{dR} (PF) = 0$$

or

$$\frac{d(\ln PF)}{d(\ln R)} = -3\left(1+\frac{Q}{PF}\right).$$

In the strong shock regime we found that F was essentially constant and $Q \sim P$. Therefore, in this regime $Q/PF \sim$ constant. In the weak shock regime, $Q \sim P^3$, $P \sim R^{-1}$ and with $F \sim R^{-2}$ the ratio Q/PF is again

essentially constant (although not necessarily the same constant as that in the strong shock regime); thus

$$\ln Q = \ln \text{constant} + \ln PF.$$

Denoting $3(1 + Q/PF)$ by q, leads to

$$-q = d[\ln Q - \ln \text{constant}]/d(\ln R)$$

or

$$-q = d(\ln Q)/d(\ln R) .$$

Integration of this equation produces the result that

$$QR^q = \text{constant}. \tag{36}$$

Lastly, we note that R^3 and Z^3 differ by an additive constant, hence, their derivatives are equal. The result is that by replacement of derivatives, integration and change of the constant,

$$QZ^q = \text{constant}. \tag{37}$$

We require estimates for the constant q in the strong and weak shock regimes. It can be shown that the above equations lead to

$$\frac{d(\ln Y)}{d(\ln R)} = 3 + \frac{d(\ln PF)}{d(\ln R)} = 3-q$$

Additionally, Equation (20b) leads to the suggestion that

$$\frac{d(\ln Y)}{d(\ln R)} \sim -1$$

in the strong and weak regimes. In the weak regime all of the prompt

energy is subject to waste; however, in the strong regime only one half the prompt energy is subject to waste. Hence, we expect

$$\frac{d(\ln Y)}{d(\ln R)} \sim \begin{cases} -1 & \text{weak regime,} \\ -\frac{1}{2} & \text{strong regime.} \end{cases}$$

These estimates are borne out by detailed calculations[8] thus, we accept the values of q as

$$q = \begin{cases} 4.0 \text{ weak,} \\ 3.5 \text{ strong.} \end{cases}$$

C. PEAK OVERPRESSURE CALCULATION SCHEME (POCS)

The necessary technical arguments are in position to show how to make a simple scheme for calculation of spherical blast wave overpressure. The interior analyses give rise to an estimate for the initial yield and an initial radius for the charge can be determined by 1/6 of the propellant mass and the specific gravity of the propellant. All that remains is determination of the constant in the QZQ hypothesis.

Since QZ^q is constant for all Z we shall select the transition radius, that is, the radius at which the shock wave changes from strong to weak, as the point at which the constant shall be evaluated. Since the initial yield and radius are determined, Equation (20a) can be used in the form

$$Y_o = 4\pi \int_{Z_o}^{Z_t} Qz^2 dz + \int_{Z_t}^{\infty} Qz^2 dz \tag{39}$$

where Z_t is the transition radius.

The constants are different in the strong and weak regimes so let us write

$$\text{Strong:} \quad QZ^{q_1} = A = Q_t Z_t^{q_1}$$

$$\text{Weak:} \quad QZ^{q_2} = B = Q_t Z_t^{q_2}$$

Equation (39) becomes (using dimensionless energies indicated by the asterisks)

$$\frac{Y_o^*}{4\pi} \int_{Z_o}^{Z_t} A^* z^{2-q_1} dz + \int_{Z_t}^{\infty} B^* z^{2-q_2} dz .$$

This is readily integrated to give

$$\frac{Y_o^*}{4\pi Q_t^*} = \frac{Z_t^{q_1}}{3-q_1} \left[Z_t^{3-q_1} - Z_o^{3-q_1} \right] - \frac{Z_t^3}{3-q_2} \tag{40}$$

since q_2 is greater than 3. If X is defined as $X = Z_t/Z_o$ then we can write Equation (40) as

$$\frac{Y_o^*}{4\pi Q_t^* Z_o^3} = \frac{X^{q_1}}{3-q_1}\left[X^{3-q_1}-1\right] - \frac{X^3}{3-q_2} . \tag{41}$$

This equation, once Q_t^* is specified, can be solved approximately by a variety of techniques. (See, for example, Schaumm's "Numerical Analysis"[14]).

Equation (30), when combined with Equation (31), gives an expression for Q* in terms of the pressure ratio, P_r. A unique specification for the pressure at the transition point is not possible because of a variation in the criteria used to differentiate strong from weak shock waves. For example, at a pressure ratio of 3.8×10^5 pascals (3.8 atm.) the sound velocity equals the material velocity behind the shock wave and this is a good dividing point between strong and weak shocks. Another reasonable division is at the place where that pressure ratio which separates ΔP_r as greater or less than P_a. This occurs at a pressure ratio of 1×10^5 pascal (1 atm.). Around a pressure ratio of 2×10^5 pascals (2 atm.) the negative phase first develops thereby preventing any further energy from propagating from the interior to the shock wave. For lack of any definitive criteria for transition from weak to strong shocks we select a pressure ratio of 2×10^5 pascals. The waste heat at the transition point is then found to be

$$Q_t^* = .096. \tag{42}$$

In conjunction with equation (30), (31), and (41), the pressure ratio is obtained from

$$Q^* Z^{q_i} = .096(XZ_o)^{q_i} \tag{43}$$

for values of q_i of 3.5 or 4 depending upon whether Z is greater or less than Z_t ($Z/Z_o \gtrless X$).

---

[14] *F. Scheid, "Theory and Problems of Numerical Analysis," Schaum's Outline Series, McGraw-Hill Book Co., New York, (1968).*

D. ASPHERICAL GEOMETRY

The previous analyses assume spherical symmetry since most explosions can be idealized as emanating from a point source. The gases exiting from a gun would probably be conical or cylindrical in shape owing to the basic shape of the barrel and the boundary layer buildup. We wish to examine the effect of a cylindrical charge verses a spherical charge upon the results. We do this by replacing the idealized point source with a line source.

The basic relation for prompt energy, Equation (20a), becomes, for a line source,

$$Y_o = 2\pi h \int_{Z_o}^{\infty} Qz\,dz$$

where quantities are assumed constant along the line length, h. If we assume, for the moment, that the exponents, q, are the same in both strong and weak regimes this equation integrates to

$$Y_o = \frac{2\pi h K Z_o^{2-q}}{q-2}$$

since, as before, q is greater than 3. Setting K equal to the values at the transition radius and denoting the dimensionless ratio $(Z_t/Z_o)_{cyl} \equiv \xi$ and $(Z_t/Z_o)_{sph} \equiv \eta$ we find that, for equal initial yields

$$\frac{2\pi h Q_t Z_{o_c}^{2} \xi^{q}}{q-2} = \frac{4\pi Q_t Z_{o_s}^{3} \eta^{q}}{q-3}$$

or

$$\left(\frac{\xi}{\eta}\right)^q = \frac{2\ Z_{o_s}^{3}\ (q-2)}{Z_{o_c}^{2}\ h\ (q-3)} \quad .$$

Since the initial volumes must be equal, i.e., $\pi Z_{o_c}^{2}\, h = \frac{4}{3}\pi Z_{o_s}^{3}$, one has

$$\left(\frac{\xi}{\eta}\right)^q = 2\left(\frac{3}{4}\right)\frac{(q-2)}{(q-3)} \quad ,$$

or

$$\frac{\xi}{\eta} = \left[\frac{3}{2}\,\frac{q-2}{q-3}\right]^{1/q}.$$

We are left with estimating the initial radius of the clyinder with respect to that of the sphere. In the next chapter we will show that the ordered motion is approximately equal to the random motion, hence, energy transport along the axis of the barrel would be greater than the transverse flux by a factor of two. This suggests an aspect ratio, h/Z, of 2 and, since the volumes must be equal, we obtain

$$Z_{o_c}{}^3 = \frac{2}{3}\, Z_{o_s}{}^3$$

or

$$Z_{o_c}/Z_{o_s} \sim .8735.$$

Consequently,

$$Z_{t_c} \sim .8735\left[\frac{3}{2}\,\frac{q-2}{q-3}\right]^{1/q} Z_{t_s}\,. \tag{44}$$

This function is plotted in Figure 5 and shows that the transition radius is from 1.5 to 2.5 times farther away when the initial energy release is cylindrical rather than spherical in shape.

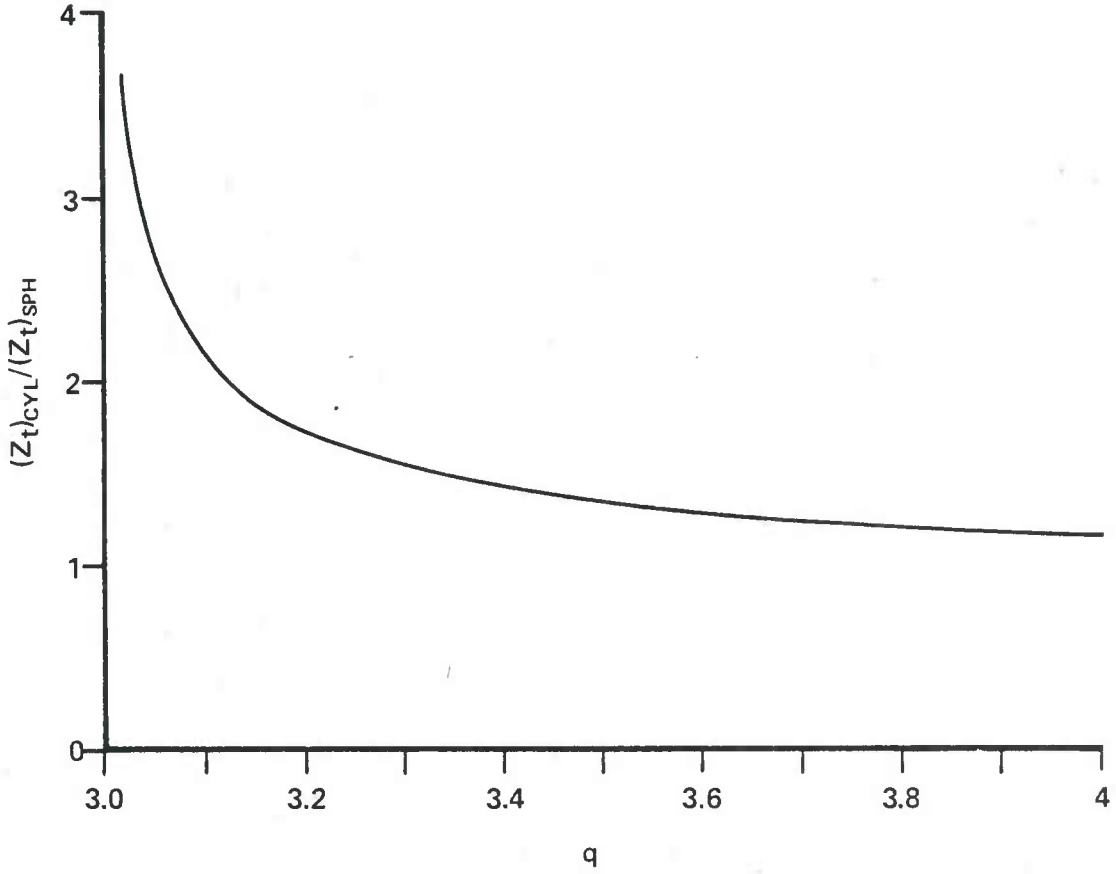

Figure 5. Cylindrical charge contribution to transition radius scaling

E. PULSE LENGTH DETERMINATION

The traditional analysis to determine the blast pulse length uses an assumed pressure pulse time history and empirical blast data. Pulse shapes ranging from polynomials (including instant-rise/linear-decay triangles) to the product of polynomials and exponentials are commonly used. A classical example is the Friedlander equation as found in Baker[6]:

$$P(t) = P_a + P_p\left(1 - \frac{t}{t_+}\right) \exp(-bt/t_+).$$

In the usual analysis the four constants P_a, P_p, t_+ and b are determined (as a function of charge weight and distance from the charge) empirically.

Another approach is that of Theilheimer[6]. He uses a pulse shape of the form

$$P(t) = P_a + P_p \exp(-t/\Theta)$$

where the time constant is defined by

$$\Theta = -\left(\frac{P-P_a}{\partial P/\partial t}\right),$$

evaluated at $t = 0_+$. Using this pulse shape and the partial differential equations that: govern the conservation of mass and momentum; define the speed of sound; and describe the change of (energy) state in an adiabatic expansion, Theilheimer finds the partial derivative of pressure with respect to time as

$$\frac{\partial P}{\partial t} = \frac{U\left\{\frac{2\rho u a^2}{R}(U-u) + \frac{dP}{dR}\left[a^2 + u(U-u)\right] + \frac{du}{dR}a^2\rho U\right\}}{a^2-(U-u)^2}.$$

The UTE could be used to determine gradients of u and P with respect to R and then to $\partial P/\partial t$ and from it, the time constant for decay of pressure at fixed distances from the blast center. However, the data currently available on durations does not justify this close examination.

In order to apply the UTE to pulse length calculation without resort to a complex computation (which is not justified by the quality of the

data) we note that the theory as presented is not time dependent; however, it can be extended for estimating the pulse length. We begin by observing that a time can be determined using a characteristic length associated with the energy volume and the material velocity. Additionally, one can relate the pressure volume energy to the prompt energy.

Let us define the pulse length by

$$\Delta t = \xi/u$$

where ξ is representative of the volume occupied by the pressure energy. We define ξ by

$$\frac{4}{3}\pi\xi^3 = \frac{4}{3}\pi\frac{\Delta v}{v_o}R^3.$$

In general then (from Equation (35))

$$Yh(e) = \frac{4}{3}\pi\frac{v_o}{\Delta v}\xi^3 p$$

where h(e) modifies the yield to include only that portion which appears as pressure energy.

The volume ratio (because of the per unit mass definition) becomes

$$\frac{v_o}{\Delta v} = \frac{1}{1-\frac{v}{v_o}} = \frac{D}{D-1}$$

where $D = \rho/\rho_o$. The form adopted for h(e) is arrived at as follows:

The prompt energy is defined as the static overpressure energy (internal energy, e_I) plus the kinetic energy. Since the kinetic energy is not detected by a static pressure probe we must reduce the prompt energy by the ratio:

$$\frac{\Delta e_I}{\Delta e_I + \Delta(u^2/2)}.$$

This can be written as

$$\frac{1}{1 + \frac{\Delta(u^2/2)}{\Delta e_I}}$$

and, since we have assumed a perfect gas, constant total enthalpy allows us to write the ratio as

$$\frac{1}{1 + \frac{\Delta h}{\Delta e_I}} \quad .$$

The ratio of the enthalpy to internal energy is recognized as the ratio of the specific heats, γ; hence, the correction factor for the prompt energy becomes

$$h(e) = \frac{1}{1+\gamma} \quad .$$

The pulse length becomes

$$\Delta t = \frac{1}{u} \left(\frac{(D-1)Y}{\frac{4}{3}\pi(1+\gamma)PD} \right)^{1/3} \quad . \tag{46}$$

III - COMPARISON OF THEORY AND EXPERIMENT

The theory which we have presented raises many questions concerning the assumptions and the ultimate validity of such an approach. In this section we shall examine data for three guns in the Army inventory and compare these data to our theory. The guns considered and the relevant characteristics are given in Table I. (We apologize for the inconsistent units; however, this is the way data is usually presented[15,16]).

Table 1

(a) Gun

Designation	Type	Barrel Length(m)	Dia.(mm)	Groove Height(m)	Propellant
XM204	towed howitzer	3.55	105	$3.5\text{x}10^{-3}$	M30A1
M110E2	self-propelled howitzer	6.93	203	$3.66\text{x}10^{-3}$	M188E2
M107	self-propelled artillery gun	8.95	175	3.66E^{-3}	M6

(b) Propellant

	Specific Gravity(g/cc)	Specific Energy(cal/g)	Chamber Temp(K)	Chamber Press.(psi)	Weight/zone (lbs)/(non-dim)
M30A1	1.66	975	3040/2450	54000	4.42/8
M188E2	1.66	975	3040/2450	31000	38/8
M6	1.58	758	3040/2450	46000	57/3

---

[15] *B.L. Reichard, A.R. Downs, "A Compendium of Field Artillery Facts - Organization, Tactics, Operations, Weapon Systems and Terminology," BRL Report No.* 1759, Feb 1975. (AD #B002431)

[16] *"Interior Ballistics of Guns," Engineering Design Handbook, AMC Pamphlet No. AMCP 706-150, Feb., 1965.*

Table 1 (Cont)

(c) Projectile

Gun	Weight(lbs)	Muzzle Vel(ft/sec)
XM204	33	2133
M110E2	200	2330
M107	147.5	3000

A. APPLICATION OF SPHERICAL EXPLOSION THEORY TO MUZZLE BLAST OVERPRESSURE PREDICTION

The overpressure theory of the previous chapter is not directly applicable to the muzzle blast problem. In this section we shall develop those adjustments, based upon preliminary examination of the data, to make the principal result, the QZQ hypothesis, applicable. In this section we shall address three areas: (1) the effect of the ordered motion of the propellant gases, (2) revised estimates for the exponents in the QZQ hypothesis and (3) the effect of the cylindrical vs. spherical initial shape. Finally, we shall illustrate our findings by using the 175mm M107 artillery gun.

A.1 The Moving Charge Effect

Energy transport in any direction is determined by the sum of ordered and random motion, each contributing according to their respective velocities. The gases issuing from a gun have velocities given by the projectile muzzle velocity, which is on the order of 3 times the speed of sound; hence, it is instructive to examine the relative significance of these motions. Experimental investigations into the effect of motion on blast overpressures were performed by Patterson and Wenig[17], Armendt[18] and Armendt and Sperrazza[19]. Their results showed that blast overpressures were measureably greater at a given distance from detonation in the direction of motion as compared to the transverse direction. We expect a similar effect in muzzle blast and in the following we give a simple procedure for including this effect.

We begin with a comparison between the energies of random and ordered motion. The kinetic energy of ordered motion is simply

$$\frac{1}{2} u^2_{\text{muzzle}}$$

---

[17] *J.D. Patterson, J.Wenig, "Air Blast Measurements Around Moving Explosive Charges," BRL Memorandum Report No. 767, Mar., 1954.* (AD #33173)

[18] *B.F. Armendt, "Air Blast Measurements Around Moving Explosive Charges, Part II," BRL Memorandum Report No. 900, May, 1955.* (AD #71277)

[19] *B.F. Armendt, J. Sperrazza, "Air Blast Measurements Around Moving Explosive Charges, Part III," BRL Memorandum Report No. 1019, July, 1956* (AD #114950)

which, for the M107, is

$$e_{\text{ordered}} \sim 4.2 \times 10^5 \text{ j/kg}$$

or

$$U_{\text{ordered}} \sim 915 \text{ m/sec} .$$

The energy in random motion is given by

$$\frac{1}{2} k T$$

per degree of freedom where k is Boltzmann's constant. Table 1 gives the temperatures as: isochoric - 3040 °K, isobaric - 2450 °K. We expect the actual temperature to be somewhere between these, hence, for convenience, let us assume the temperature to be 2750°K and an average molecular weight of 28. The energy in random motion becomes

$$\frac{1}{2} k T = 4.1 \times 10^5 \text{ j/kg}$$

which gives a random velocity of approximately 904 m/sec.

These results show that energy transport along the axis of the barrel is approximately twice that in the transverse direction. We interpret this as meaning that pressure probes, one at a distance L perpendicular to the barrel axis will sense the same pressure as one aligned along the axis at a distance L/2. For simplicity, we adjust all lengths by the factor

$$\frac{1}{1 + \cos \theta}$$

where θ is the angle between a unit vector along the barrel axis (at the muzzle) and a position vector from the muzzle to the pressure probe. This function has the characteristic of varing smoothly from 1/2 along the barrel axis to unity normal to the axis.

Figures 6a and 6b show the effect of this modification. Figure 6a shows the data as measured. The symbols denote gun elevations of : + 100 mils, □ 620 mils and ⌂ 1125 mils (military mils where 6400 mils equal 360°). The variation in each symbol is a result of different azimuth angles (0°, 30°, 60°, 90°). Application of relation (47) clearly results in a more reasonable correlation of overpressure with distance from the muzzle. For this reason all data is adjusted according to this prescription.

A.2 Revised Estimates for q

In Section II.B.5 values of 3.5 and 4 were obtained for the exponents, q, in the strong and weak shock regimes respectively. These values were predicted upon the scaling laws which state that $P \sim R^{-1}$ in the weak regime.

The previous section, III.A.1, shows that there is an effect due to the forward velocity of the gases. Since the q's relate the conversion of prompt energy to waste heat, and since the ordered motion is approximately equal to the random motion, we propose that only half of the pressure volume energy is available for conversion to waste heat. The consequence is that in the strong regime $q \sim 3.25$. Additionally, since the muzzle overpressures are relatively low (compared to H.E. explosives) the transition radius is small compared to the distances of interest. Hence, the motion effect has not disappeared and we plausibly expect the weak regime q to be approximately 3.25 also.

This conclusion is demonstrated in Figure 7 where we have plotted -ln Q vs. ln R (or ln Z since they are approximately equal far from the muzzle) for the adjusted data of Figure 6b. The straight line is a least squares regression fit of the form ax^b. The fit is to the increasing data; the points at the greatest distances were not included since they are at essentially constant pressure and do not reflect the dynamics of the processes. For these data a slope of approximately 3.2 was found. This is consistent with our assertion and demonstrates that the division of energy in crossing the shock wave is significantly affected by the existence of the ordered motion.

In our analyses we shall use equal q's of value 3.25.

A.3 Initial Cylindrical Shape

In Section D of the previous chapter we developed

$$(Z_t)_{cyl} \sim .8735 \left[1.5 \frac{q-2}{q-3}\right]^{1/q} (Z_t)_{sph} ,$$

DATA ADJUSTMENT FOR MUZZLE VELOCITY EFFECT
M107 ARTILLERY GUN (175MM)

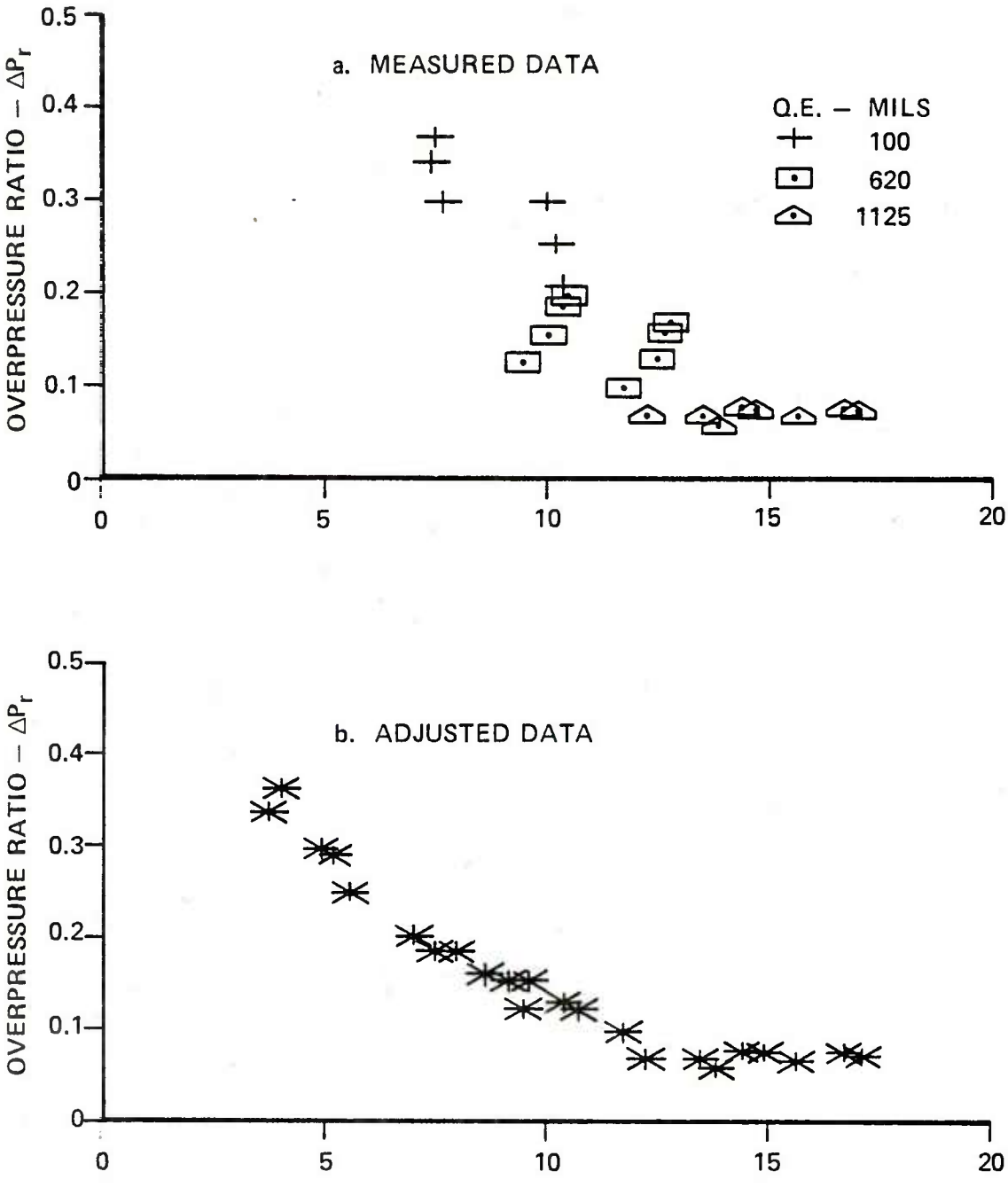

FIGURE 6

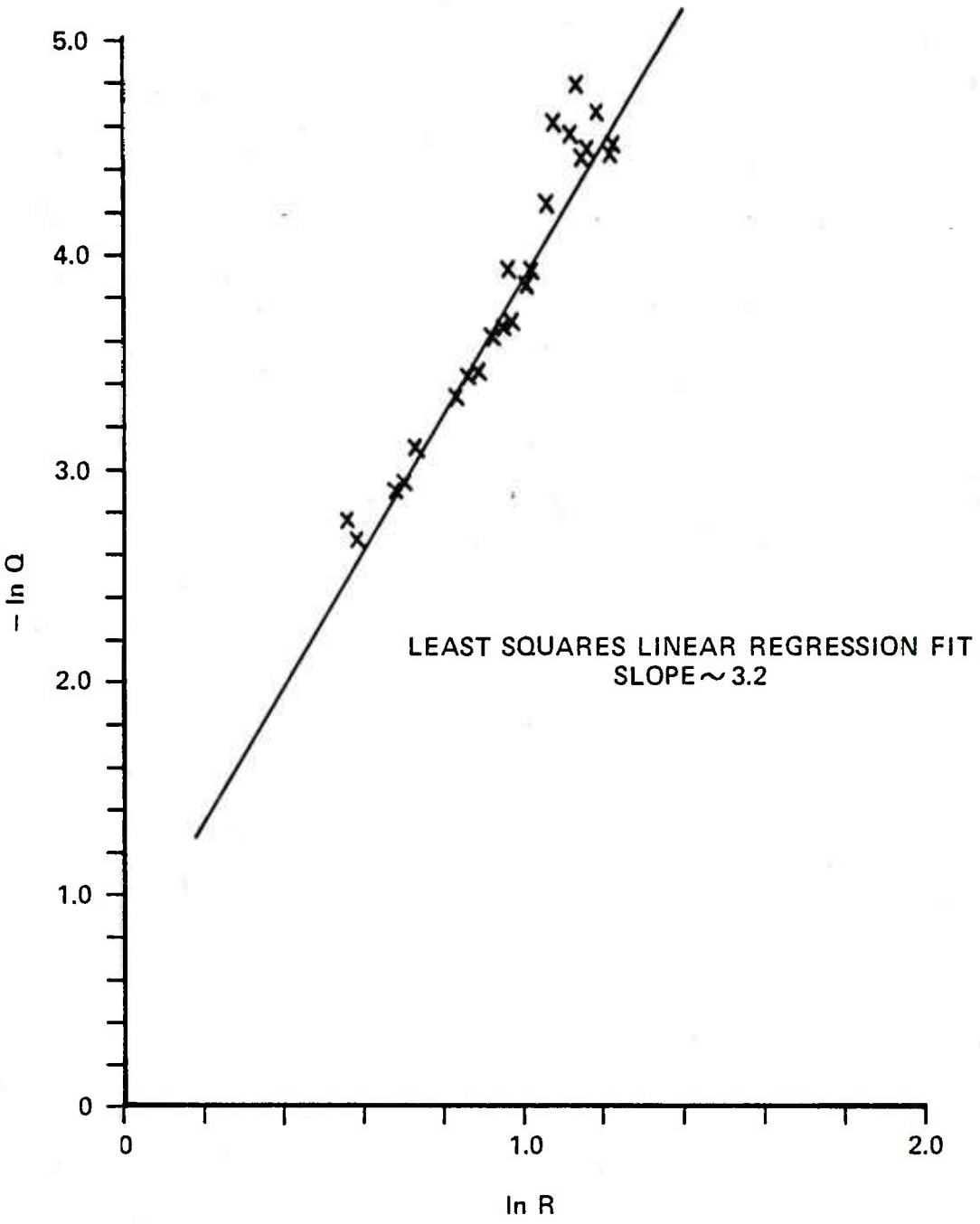
VARIATION OF WASTE HEAT WITH DISTANCE
M107 ARTILLERY GUN (175MM)
5.0
4.0
3.0
2.0
1.0
0
- ln Q
0
1.0
2.0
ln R
LEAST SQUARES LINEAR REGRESSION FIT
SLOPE ~ 3.2

FIGURE 7

a modification to the theory because of a proposed initial cylindrical shape to the charge. For a q of 3.25 we find that

$$(Z_t)_{cyl} \sim 1.624\ (Z_t)_{sph} .$$

When the transition radius is near the muzzle we still expect the cylindrical shape to be present since sufficient time has not elapsed for these asymmetrical effects to be washed out.* That the cylindrical transition radius is more appropriate is shown in Figure 8.

*For an exit Mach number of 2.3 and transition radius of 1 metre the elapsed time is of the order of 1 msec.

EFFECT OF INITIAL CHARGE SHAPE ON MUZZLE BLAST OVERPRESSURE
M107 ARTILLERY GUN (175MM)

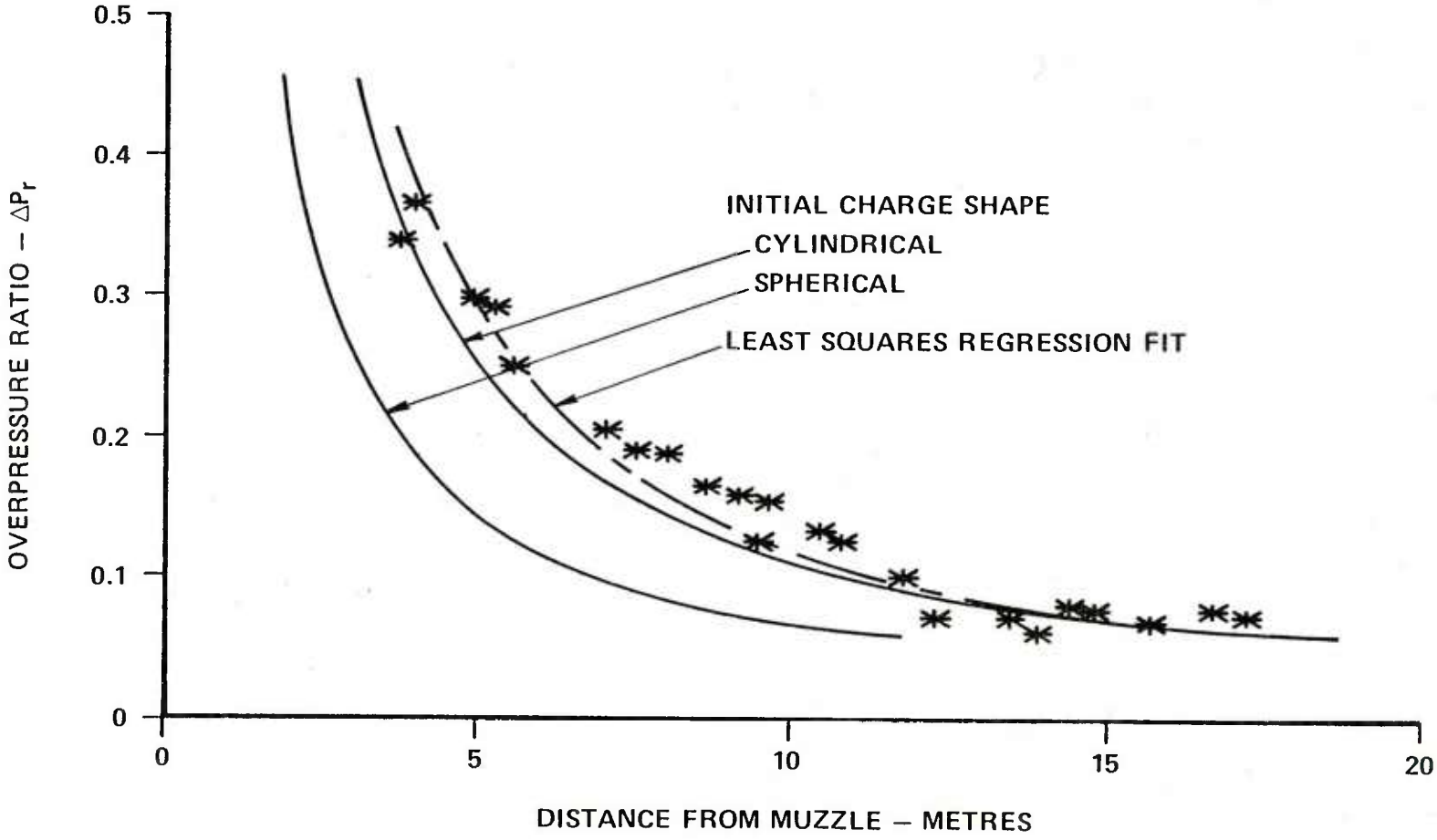

FIGURE 8

B. COMPARISON OF THEORY AND EXPERIMENT

In this section we will apply our theory to the guns described at the beginning of this section. In each case we have also provided a least squares regression fit of the form $y = a\,x^b$ to the adjusted data. The data for the M110E2 and the M107 were obtained from the Material Test Directorate at the Aberdeen Proving Ground, Md.[20] The XM204 data were obtained from Westline's report[5]. We note that the APG data error is claimed to be a maximum of $\pm$ 5%. We also note that for clarity in certain instances, data which did not add further information were not plotted.

B.1 Muzzle Blast Overpressure

Figure 8 in the previous section shows our prediction for the 175mm M107 artillery gun. For the adjusted data the regression fit yielded an exponent, b, of -1.29. The measured data are: + - 100 mils quadrant elevation (Q.E.), □ - 620 mils Q.E., and ⌂ - 1125 mils Q.E. Additionally, each symbol includes variation in the azimuth at values of 0°, 30°, 60°, and 90°. Two probes were located at each of the angles on circular arcs of radii 9.15 and 12.2 metres from the muzzle when at a Q.E. of 100 mils.

Within the data field a maximum disagreement (in overpressure ratio) between the theory and data is found to be approximately +15%. This corresponds to a 3.9% error in the absolute pressure.

Figures 9a and b show the data and theoretical prediction for the M110E2 self-propelled howitzer. Figure 9a shows the measured data with the symbols denoting the same conditions as with the M107.

Figure 9b shows the adjusted data, the theoretical prediction and the least squares regression fit. The regression fit gave an exponent, b, of approximately -1.26. In this fit the two flagged points were not included. These points correspond to a Q.E. of 100 mils with the probes located directly in front of the muzzle (0° azimuth). These abnormally low overpressures may be attributed to the losses associated with the flow patterns, i.e., the normal shocks associated with the Mach disks, and hence, are not characteristic of the overall decrease of pressure with distance. This assertion cannot be validated since similar data were not observed with the other guns examined. We can state that since the basic reason for this paper is predication of overpressures for safety reasons, these low values are of no consequence for the work at hand.

---

[20] *D. Lacy, Private Communication.*

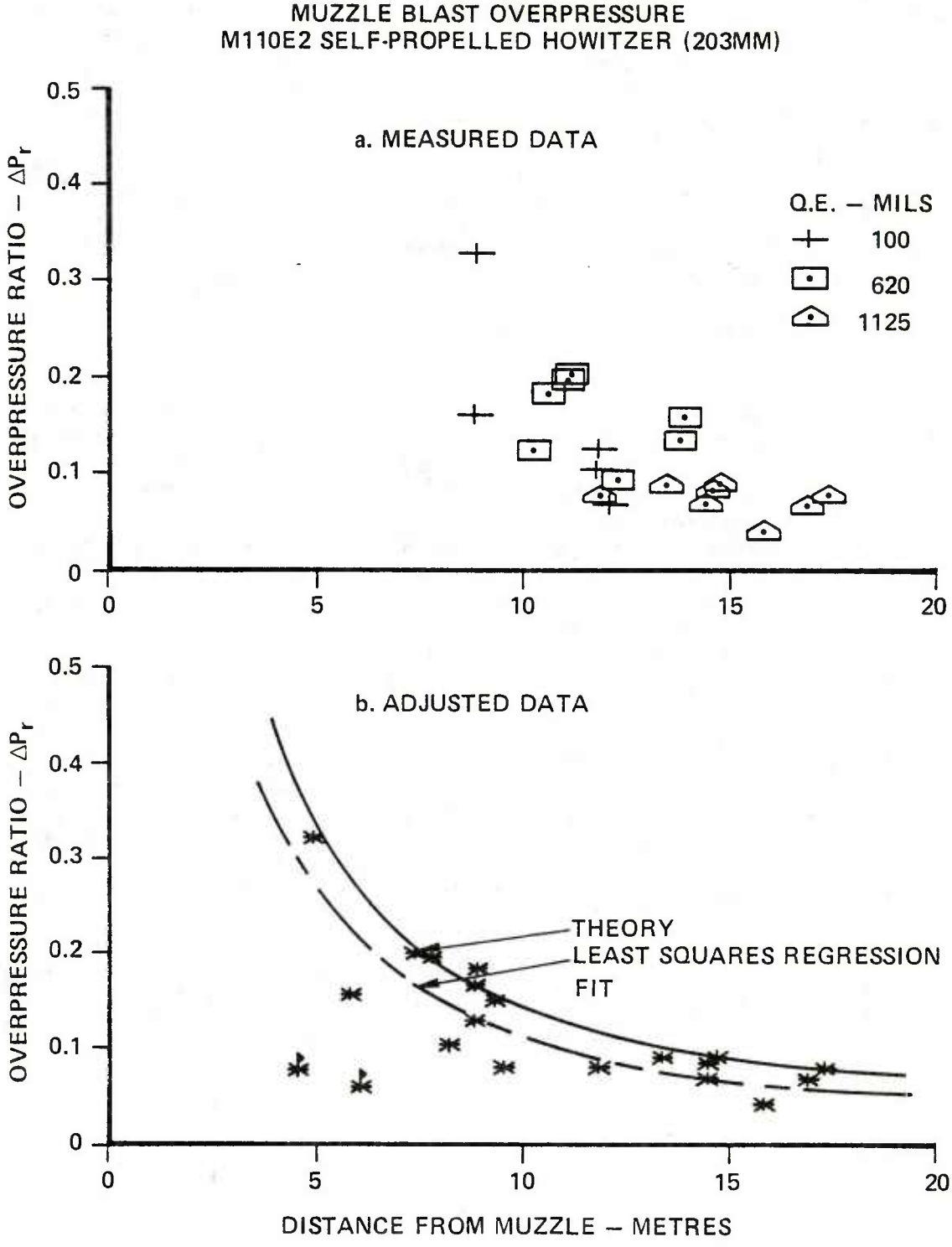
MUZZLE BLAST OVERPRESSURE
M110E2 SELF-PROPELLED HOWITZER (203MM)
a. MEASURED DATA
Q.E. – MILS
100
620
1125
OVERPRESSURE RATIO – ΔP_r
0.5
0.4
0.3
0.2
0.1
0
0
5
10
15
20
b. ADJUSTED DATA
THEORY
LEAST SQUARES REGRESSION FIT
DISTANCE FROM MUZZLE – METRES

FIGURE 9

For these M110E2 data the theoretical prediction is upwards of +25% in error for the overpressure ratio (compared to the regression fit). This corresponds to approximately 5.2% in absolute pressure.

Figures 10 a and b show the data for the XM204 towed howitzer. Figure 10a shows the measured data. These data were all obtained at a quadrant elevation of 26.7 mils and the data represent variation in the azimuth.

Figure 10b shows the adjusted data. For these data the theoretical prediction and the regression fit are basically indistinguishable. This figure also nicely illustrates how the data collapse about the 90° azimuth value.

B.2 Muzzle Blast Pulse Length

The data in this section represent the positive phase duration. That is, the measured data represent the time duration between the start of the pulse and the point where the initial pulse returns to ambient pressure. The range component of the duration data has been adjusted in the same way (and for the same reason) as the range component of the pressure data. But, unlike the pressure data the pulse length is adjusted in addition to the range. We argue that an observer standing in front of the muzzle will see, in time, a shorter pulse because of its velocity than an observer standing at 90° to the muzzle unit normal. We have provided the regression fit for these data; however, there is sufficient scatter in the data that both authors and readers are wise to refrain from drawing any comparisons between the theory and the fit.

Figures 11 a and b show the pulse length for the M110E2 and Figures 12 a and b show the data for the M107. The symbols correspond to the same conditions as noted for the overpressure data. Our theoretical predictions generally fall along the top of the measured data.

We have not examined the XM204 pulse length data because of difficulties in interpreting the exact nature of the data.

Lastly, Figure 13 shows the M107 overpressure data again, this time including bars to denote the stated error of +5%. We show this to reaffirm the discussion which compared our theory to the regression fit.

MUZZLE BLAST OVERPRESSURE
XM204 TOWED HOWITZER (105MM)

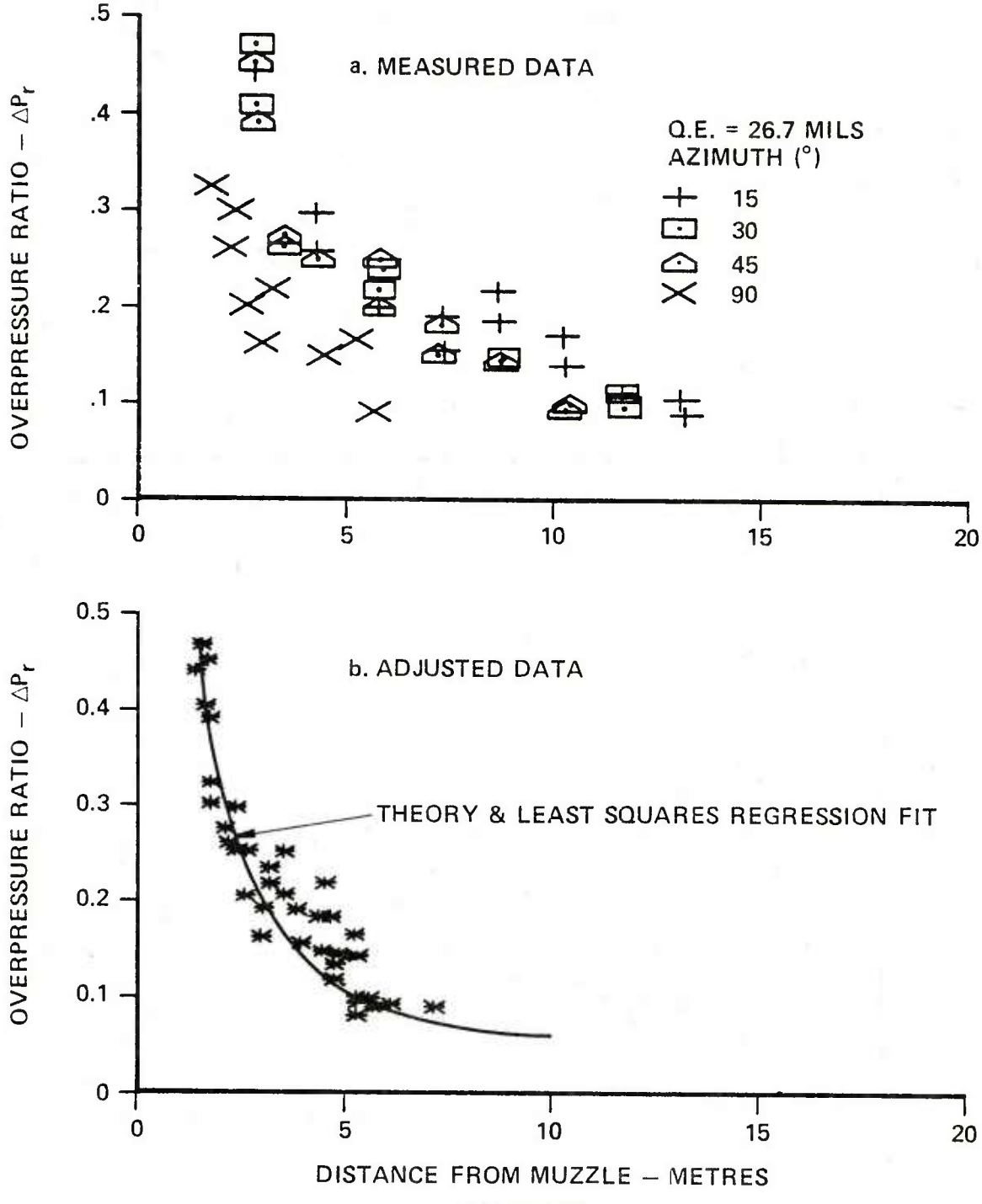

FIGURE 10

MUZZLE BLAST PULSE LENGTH
M110E2 SELF-PROPELLED HOWITZER (203MM)

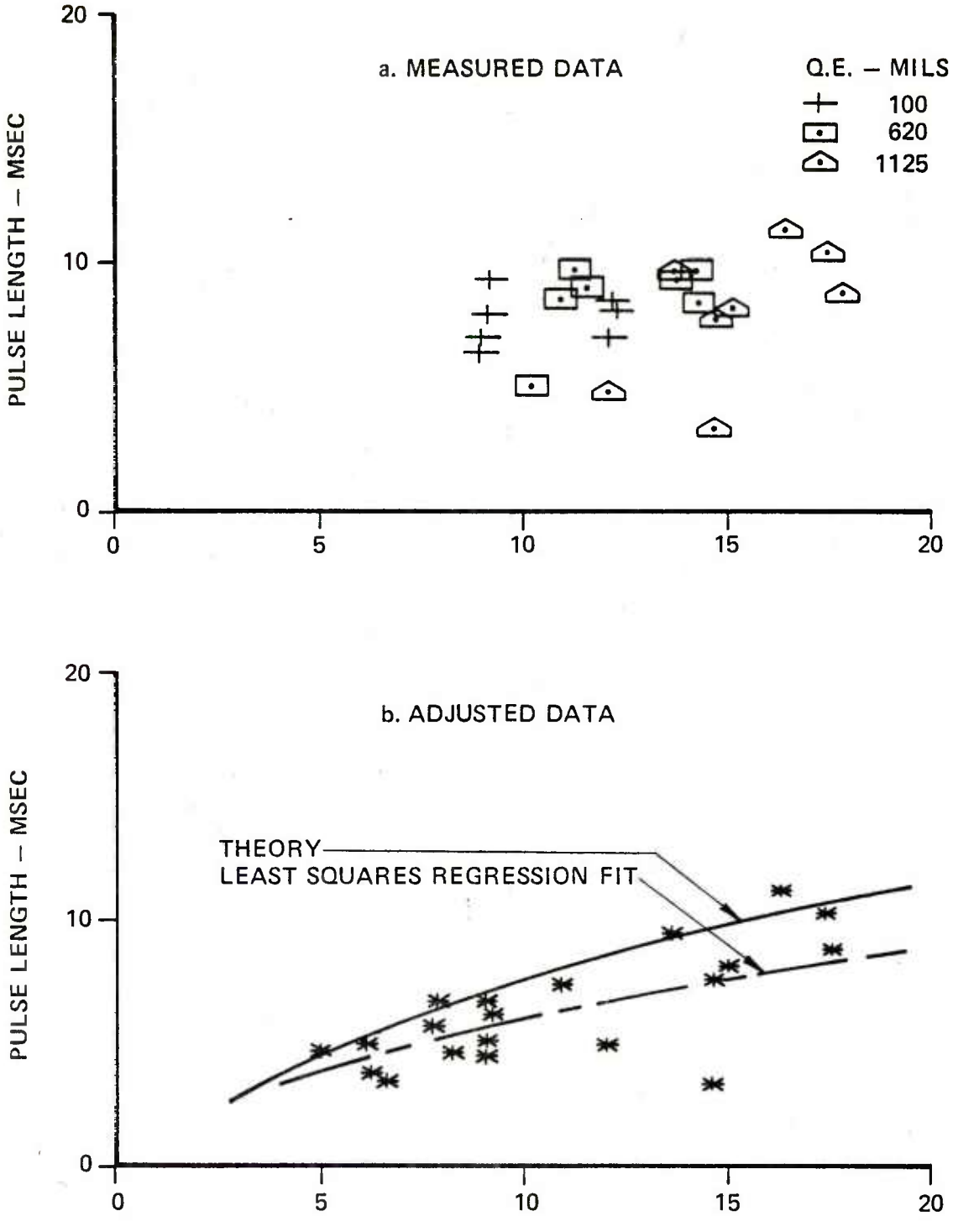

FIGURE 11

MUZZLE BLAST PULSE LENGTH
M107 ARTILLERY GUN (175MM)

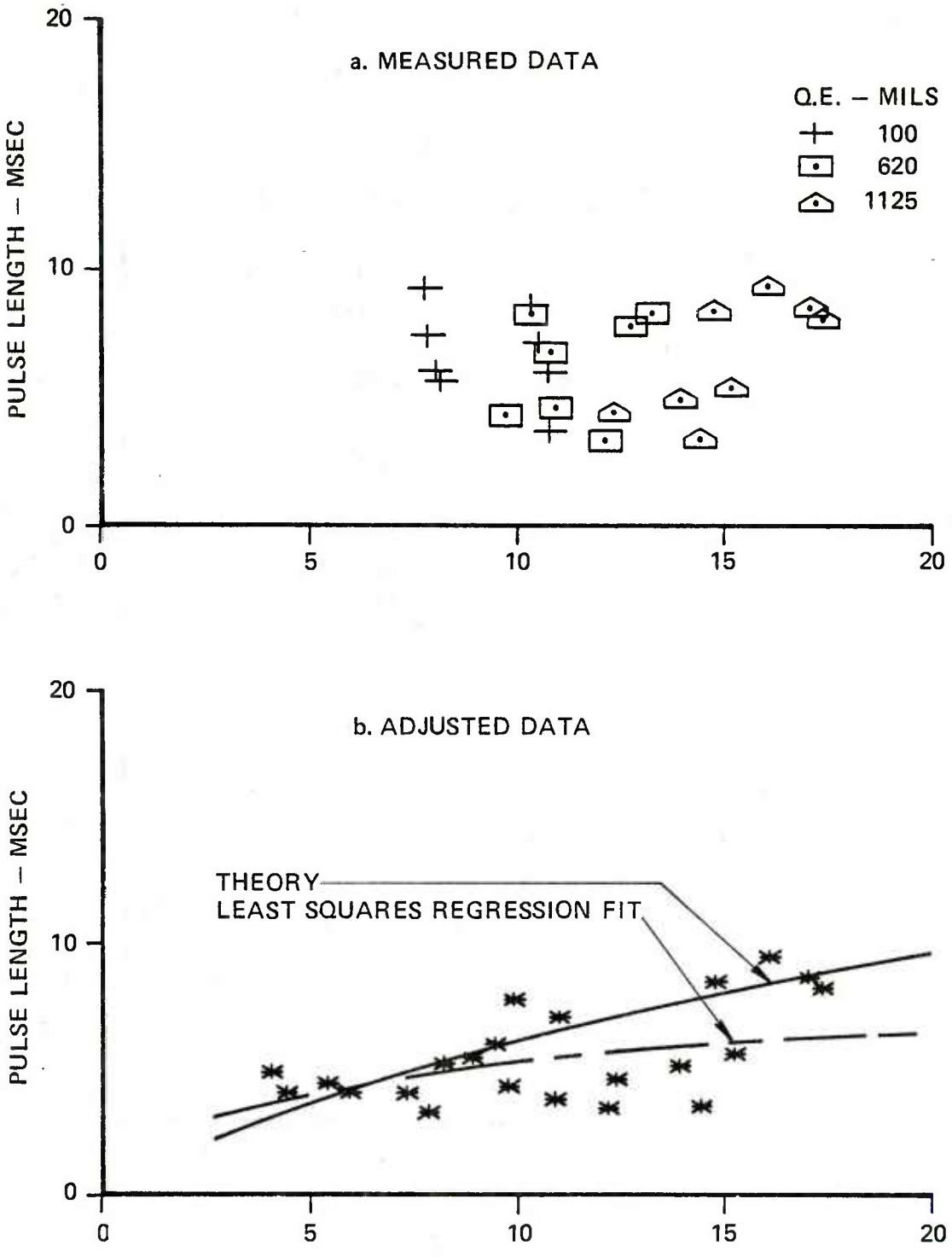

FIGURE 12

MUZZLE BLAST PEAK PRESSURE
M107 ARTILLERY GUN (175MM)

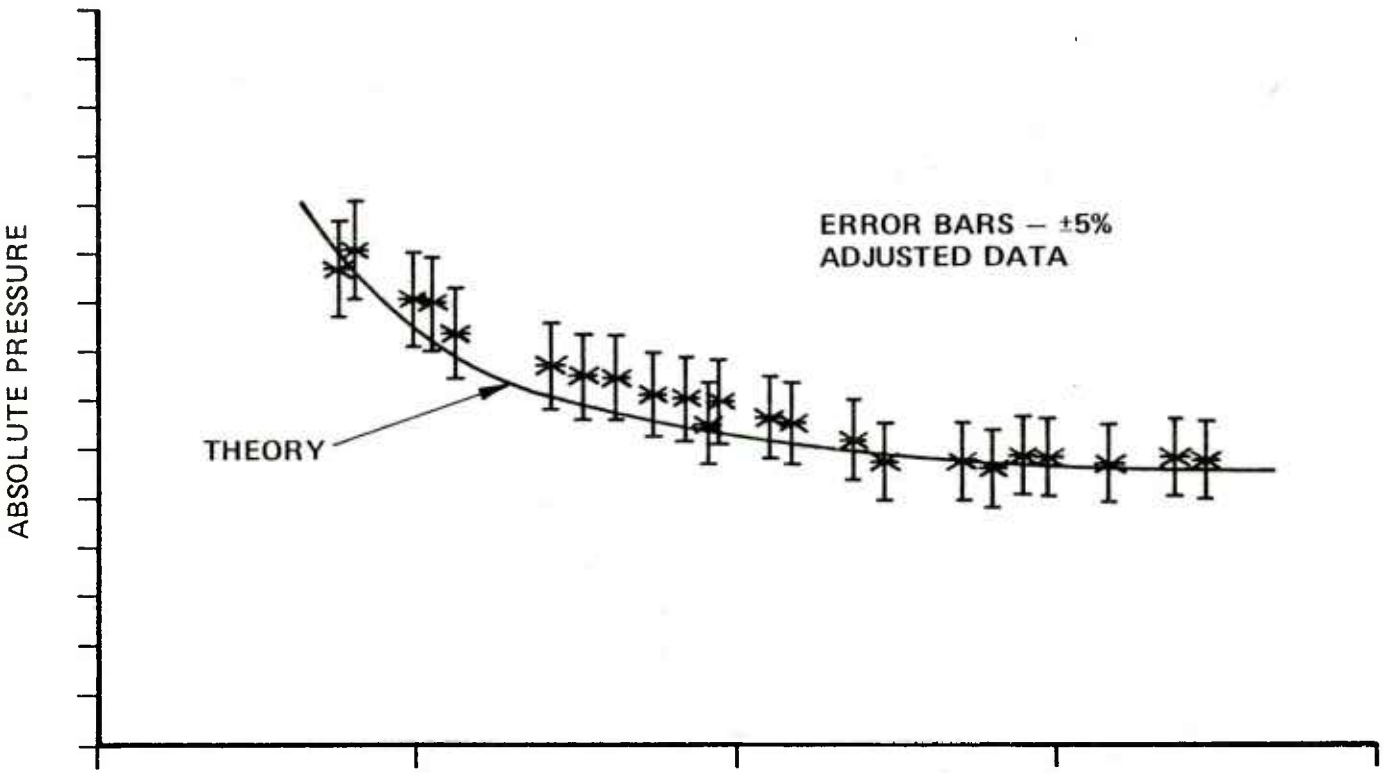

FIGURE 13

C. DISCUSSION

In view of our results, specifically with regard to the modification for cylindrical geometry, we can form a tentative picture of the gross features of the muzzle blast flow field.

Perhaps the most unrealistic characteristic of the assumed cylindrical shape is the requirement of constant pressure along the length of the cylinder. An examination of the expected processes in the flow field show that this may well be true. Previously we spoke of the inter-relationship between the static and dynamic pressures *ala Bernoulli*. In those discussions we used the Bernoulli principle to arrive at the projectile base static pressure. Once the gases have left the muzzle the reverse process must occur. That is, the high dynamic pressure of ordered motion must revert to static pressure as the gases decelerate to zero velocity. This velocity decrease will occur along the axis of the gun hence we should expect a production of pressure energy along this line--forming a more cylindrical, rather than spherical, shape.

This energy conversion produces a second, equally important effect. Classical explosion theory assumes an instantaneous point source explosion. Porzel's theory admits of afterburning* by permitting q's below his suggested values but we found that even reducing the exponent's value to the minimum (lower bound of 3) did not produce the necessary change in the slope of the pressure curve. This production of pressure energy persists for such sufficiently long times compared to ordinary explosions, that this pressure energy production continues to feed the shock wave long after the weak shock regime has been entered, as is demonstrated in Figure 14.

Figure 14 shows the absolute peak pressure plotted against the range. We applied a least squares linear regression fit to the decreasing pressure data and found a slope of approximately -.5. This is half that determined for standard spherical explosions and is indicative of some more or less continuous source of pressure energy addition to the shock front.

One might alternatively view this in light of the concepts of prompt energy and waste heat. We have noted that the kinetic energy is not subject to waste. In the muzzle blast problem we have a large reservoir of kinetic energy due to the initial high velocity of the gases; because of this resevoir the energy division suggested by Rankine-Hugoniot relations is not valid.

*A process of continued energy addition to the shock front.

LINEAR REGRESSION FIT TO MUZZLE BLAST PEAK PRESSURE
M107 ARTILLERY GUN (175MM)

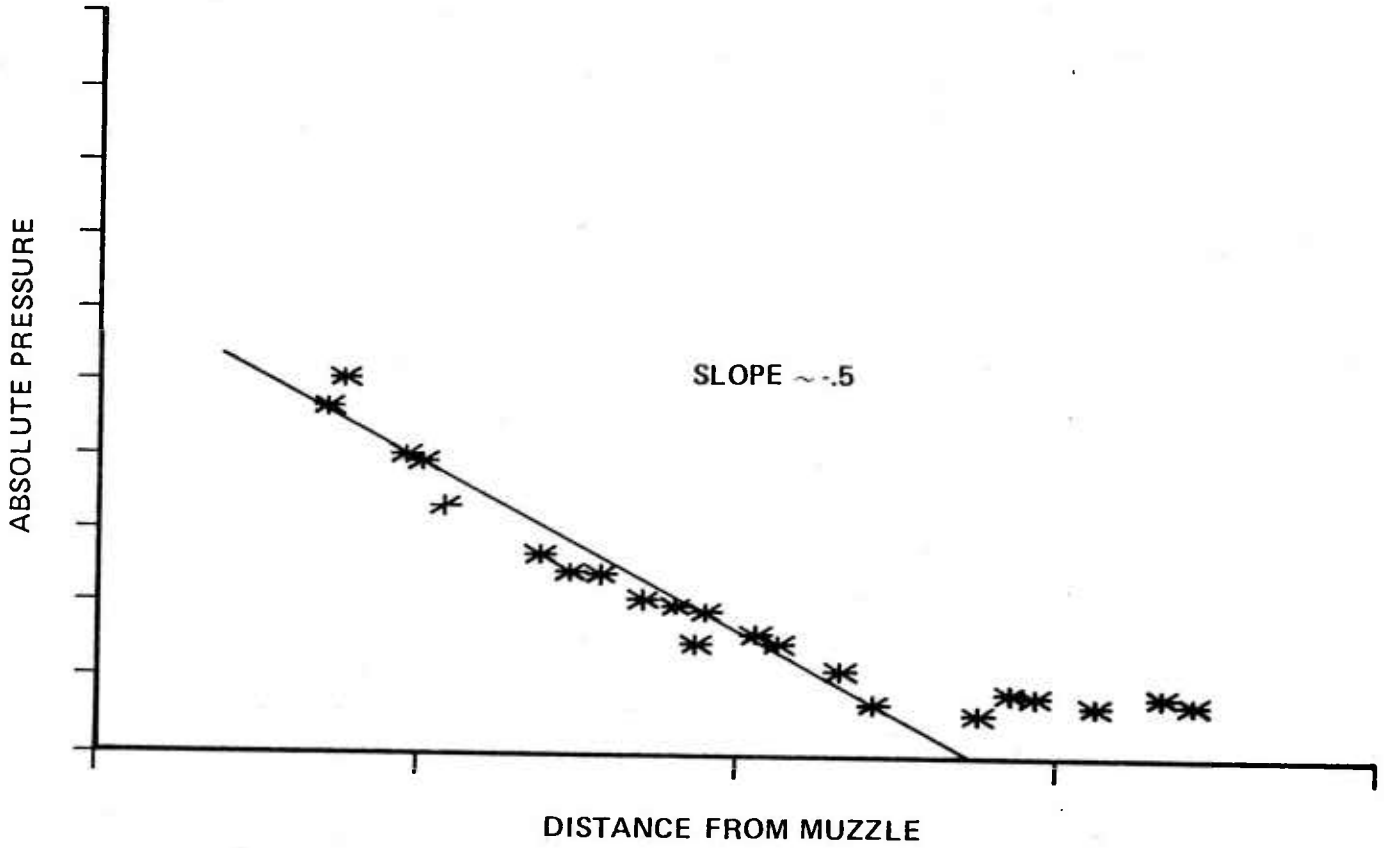

FIGURE 14

D. SUMMARY AND CONCLUSIONS

In general the *a priori* muzzle blast theory is viable. Overpressure prediction agrees with the adjusted data to within the stated error in data. The pulse length prediction generally follows the upper (longer) pulse length data which, for safety requirements, is a most desirable attribute. We note that there is sufficient scatter in the pulse length data that further, more refined experimentation is warranted before complete confidence is obtained. In this regard, more detailed study of Porzel's theory in deriving the constant may be justified, as suggested in Section II.E.

At the outset, we suggested that a detailed knowledge of the flow field is not necessary. This has been demonstrated for the data examined. We recognize that all the data occurred in the weak shock regime; had strong shock regime data been available, we would have expected a departure of this theory from experiment - a consequence of the detailed flow field. We would expect the theory to overpredict since there are losses in the muzzle flow field not accounted for in the UTE. We do note that the transition distance separating the strong from the weak regime was consistently less than one metre, a data source for R < 1m would not likely be found.

We have examined three guns of sufficient variation in length, loading etc., to span the data field for large guns and therefore, the theory can be reasonably applied to any large gun in the Army inventory, but only within the constraints of our analysis.

We have not examined the small gun effects - an area we leave for further application of the theory.*

The most striking result of this investigation is the difference in the behavior of the shock overpressure with distance between the guns examined and that which results from conventional point source explosions. The energy partition concepts suggest that a significant reduction in overpressure can be achieved by introducing some effective means for converting this high dynamic pressure to static, or random motion, early in the propagation phase.** The implementation of such a device would probably increase the overpressure near the muzzle but, since higher overpressures mean higher losses, less energy would be available in the shock as it leaves the immediate vicinity of the muzzle. Considerable reduction in the overpressure can be achieved if the range dependence can be made to more closely approximate the point source dependence, i.e., R^{-1}.

*See next section for recommended future studies.

**In small arms, noise suppressor (silencers) do exactly this through a throttling process.

This report presents a theory which is applicable to the muzzle blast problem for the situations considered. Several variations were not examined. The next section suggests future studies with, in some instances, possible techniques for including the additional effects.

E. SUGGESTED FUTURE STUDIES - AREAS NOT CONSIDERED IN THIS STUDY

1. Small Arms - We know of no *a priori* reason why the theory would not be directly applicable. One possible exception would occur if the gun L/D becomes less than the L/D for the boundary layer choke. Should this occur, we believe the muzzle velocity of the bullet, and hence the exhaust gases, will be indicative of the energy reduction from the chamber pressure.

2. Muzzle Brakes - We view this as strictly an energy, mass, and flow symmetry diverter. It is probable that most of this effect can be included in MEZ and the initial yield estimate. However, an appropriate trigonometric function describing the additional variations in angle about the barrel axis will be required.

3. Reflected Shocks - (a) from the ground. One possibility is to double the initial yield input to the calculation. Another is to provide an accelerated rate of conversion of kinetic energy of ordered motion to random motion at the various ranges. (b) from structures such as gun mounts. Detailed analysis near the structure would be very complicated because of the geometry of the structure itself. Away from the structure, however, local spatial variations should smooth out. Perhaps introducing a cylindrical explosion of shape equivalent to the structure would provide a start. As with the current problem, an estimate for the equivalent yield would probably be the more difficult task.

4. Lastly, we would like to see more refined tests so a better evaluation of this theory can be made.

REFERENCES

1. E.M. Schmidt, R.E. Shear, "The Flow Field About the Muzzle of an M16 Rifle," BRL Report No. 1692, Jan., 1974. (AD #916646L)

2. E.M. Schmidt, R.E. Shear, "Launch Dynamics of a Single Flachette Round," BRL Report No. 1810, Aug., 1975 (AD #B006781L)

3. C.K. Zoultani, "Evaluation of the Computer Codes BLAST, DORF, HELP, and HEMP for Suitability of Underexpanded Jet Flow Calculations," BRL Report No. 1659, Aug., 1973 (AD768708).

4. J. Ranlet, J. Erdos, "Muzzle Blast Flow Field Calculations," BRL Contract Report No. 297, Apr., 1976. (AD #B011967L)

5. P.S. Westine, J.C. Hokanson, "Prediction of Stand-off Distances to Prevent Loss of Hearing from Muzzle Blast," Rock Island Arsenal Report No. R-CR-75-003, Feb., 1975 (ADIA-005274).

6. W.E. Baker, "Explosions in Air," U. of Texas Press, Austin and London, 1973.

7. G.I. Taylor, "The Formation of a Blast Wave by a Very Intense Explosion: I Theoretical Discussion," Proc. Roy. Soc., 201, 159-174, (1950).

8. F.B. Porzel, "Introduction to a Unified Theory of Explosions (UTE)," NOLTR-72-209, Sept., 1972 (AD-758000).

9. Y.B. Zel'dovich, Yu P. Kaizer, "Physics of Shock Waves and High-Temperature Hydradynamic Phenomena," Academic Press, New York and London, 1966.

10. F.B. Porzel, "Correlation of Blast Simulators with a Unified Theory of Explosions," 3rd International Symposium on Military Applications of Blast Simulators, Schwetzinger, Germany, Sept., 1972.

11. F.B. Porzel, "Study of Shock Impedance Effects in a Rough Walled Tunnel," Institute for Defense Analysis Research Paper P-330, Mar., 1969 (AD684790).

12. L.D. Landaw, E.M. Lifshitz, "Statistical Physics," Pergamon Press Ltd., London, 1958.

13. L.M. Milne-Thomson, "Theoretical Hydrodynamics," The MacMillan Co., New York, 1950.

14. F. Scheid, "Theory and Problems of Numerical Analysis," Schaum's Outline Series, McGraw-Hill Book Co., New York, (1968).

15. B.L. Reichard, A.R. Downs, "A Compendium of Field Artillery Facts - Organization, Tactics, Operations, Weapon Systems, and Terminology," BRL Report no. 1759, Feb., 1975. (AD #B002431L)

16. "Interior Ballistics of Guns," Engineering Design Handbook, AMC Pamphlet No. AMCP 706-150, Feb., 1965.

17. J.D. Patterson, J. Wenig, "Air Blast Measurements Around Moving Explosive Charges," BRL Memorandum Report No. 767, Mar., 1954. (AD #33173)

18. B.F. Armendt, "Air Blast Measurements Around Moving Explosive Charges, Part II," BRL Memorandum Report No. 900, May, 1955. (AD #71277)

19. B.F. Armendt, J. Sperrazza, "Air Blast Measurements Around Moving Explosive Charges, Part III," BRL Memorandum Report No. 1019, July, 1956. (AD #114950)

20. D. Lacy, Private Communication.

21. "Military Standard - Noise Limits for Army Material," MIL-STD-1474A(MI), 3 Mar., 1975.

Appendix - Computational tools

At the outset we sought a theory which was simple to use. In this appendix we supply two different schemes for calculating the muzzle blast overpressure and pulse length. We are presenting these different schemes because, depending upon the user and the situation, different levels of versatility may be required. These two schemes and their scope are:

(1) A code for the Texas Instruments SR-52 programmable pocket calculator. In this version all assumptions, i.e., equal q, cylindrical symmetry etc. are incorporated and combined into "lumped" constants. Changing any of the values requires considerable reprogramming. To conserve space in the machine we have applied "fits" to the transcendental equations and, additionally, the pressure ratio is input and the radius determined rather than vice versa.

(2) A code written in BASIC suitable for use on a minicomputer. Complete flexibility is permitted in this code. This program was developed on a NOVA minicomputer with 8k memory (of which the BASIC translator occupies approximately 4k).

Also, a series of nomographs will be provided under separate cover where quantities are considered together as combined variables. Their numerical values are left to the user. In the nomographs we have assumed the exponents, q, to be equal and also that the user has available some sort of calculating machine whether it be a pocket calculator or a slide rule.

These computational schemes are designed to be used with the metric system of units, specifically the mks system. To facilitate use of these codes by those not accustomed to working in these units we provide the following table:

Table App-1

Units Given	Times	Metric Units
Length ft.	3.048×10^{-1}	metres - m
Wgt/mass lbs.	4.536×10^{-1}	Kilograms - kg
Pressure psi	6.894×10^{3}	Pascals (Pa) - J/m^3
Energy ft.-lb.	1.356	Joules - J
Velocity ft./sec	3.048×10^{-1}	metres/sec - m/sec

App-1 Code for the Texas Instruments SR-52 Pocket Calculator.

This code is contained on two cards. The first program accepts the input data and calculates the yield and radius of the charge. The second program accepts the pressure ratio and determines the distance from the muzzle at which the pressure ratio occurs and the pulse length at that point. The code makes use of fits to the complicated functions to permit an estimate of the correct answer.

The analysis is as follows: (Quantities followed by (I) are input)

(1) The kinetic energy of the projectile is obtained from the mass (I) and velocity (I) of the projectile.

(2) The total energy is obtained from the mass (I) and specific energy (I) of the propellant.

(3) The difference between (2) and (1) becomes the maximum available energy.

(4) The chamber overpressure ratio (I) is used to determine the choke overpressure ratio from

$$(\Delta P_r)_{Choke} \cong \exp\left[.92\ \ln(\Delta P_r)_{Chamber} - 2.14\right]$$

(5) The barrel length (I), barrel diameter (I) and the groove height (I) are used to calculate the rough wall tube loss from

$$(\Delta P_r)_{Muzzle} = \exp\left\{\ln(\Delta P_r)_{Choke} + 1.9h\left[\left(\frac{L}{D}\right)_{Choke} - \left(\frac{L}{D}\right)_{Gun}\right]\right\}.$$

If $(L/D)_{choke}$ is greater than $(L/D)_{gun}$ the program halts with a blinking display - this analysis does not include this situation.

(6) The program then determines the yield via

$$Y_o = \left\{(\Delta P_r)_{Chamber} / \left[6 \times (\Delta P_r)_{Muzzle}\right]\right\}^{E_{Avail}} - j$$

(7) The mass correction for MEZ (Section II.B.2) is determined by

$$M' = 8.2 \times 10^{-3} M_{Prop} \qquad -m^3$$

(8) The specific gravity of the propellant (I) is used to calculate the inital radius from

$$R_o \cong \left[\frac{1}{25\rho_p} M_{Prop}\right]^{1/3} \qquad -m \ .$$

(9) The mass corrected initial radius is obtained from

$$Z_o = \left[R_o^{\,3} - M'\right]^{1/3} \qquad -m \ .$$

(10) The transition radius, Z_t, is found from

$$Z_t = Z_o\left(\frac{Z_t}{Z_o}\right) = Z_o\left(\frac{Y_o}{16\pi Q_t Z_o^{\,3}}\right)^{1/3.25} \qquad -m$$

where the value of Q_t, 9.55×10^{-2}, is found assuming an overpressure ratio of 2 at the transition point.

This concludes the calculations on card 1. Card 2 calculates the following:

(11) The uncorrected transition radius, R_t, is obtained from

$$R_t = \left[Z_t^{\,3} - M'\right]^{1/3}$$

(12) The constant in the QZQ hypothesis is obtained from

$$A = Q_t Z_t^{\,3.25}$$

for a Q_t of 9.55×10^{-2}.

(13) The program now accepts a pressure ratio (I) and calculates the distance from the muzzle at which this pressure ratio occurs via

$$D = \frac{6P_r+1}{P_r+6}$$

$$Q = 2.5\left[\frac{P_r^{1/1.4}}{D} - 1\right]$$

$$Z = \left(\frac{A}{Q}\right)^{1/3.25} = \left(\frac{Q_t Z_t^{3.25}}{Q}\right)^{1/3.25}$$

and

$$R = \left[Z^3 - M'\right]^{1/3} \times 1.624$$

(14) The program then calculates the pulse length from

$$u = 280\left[(P_r-1)\left(\frac{D-1}{D}\right)\right]^{1/2} \text{ m/sec}$$

$$\Delta t = \frac{1}{u}\left[\frac{Y_o}{\frac{4}{3}\pi(P)(1+\gamma)\left(\frac{D}{D-1}\right)}\right]^{1/3}$$

$$= \frac{1}{u}\left[\frac{5A(D-1)Z^{-.25}}{D(P)}\right]^{1/3}$$

The user instructions, required inputs and displayed quantities follow:

Step		Procedure	Enter	Press	Display
Card 1	1	Load side A		Clr 2nd Read	
	2	Load side B		2nd Read	
	3	Initialize		Clr A	0.
	4	Kinetic En. of Proj.	Proj. mass - kg	RUN	M/2
	5		Proj. Vel - m/sec	RUN	E_{proj}-j
	6	Energy in Prop.	Prop. Mass - kg	RUN	M_{prop}-kg
	7		Specific En.-j/kg	RUN	E_{avail}-j
	8	Interior losses	$(\Delta P/P_o)_{chamber}$	RUN	$(\Delta P/P_o)_{choke}$
	9		Barrel Length - m	RUN	L_{barrel}-m
	10		Barrel Dia. - m	RUN	$(L/D)_{gun}$
	11		Groove Hgt. - m	RUN	25.
	12	Yield & Rad. of Eqv. Exp.	Sp. Gravity - kg/m^3	RUN	Z_t - m
Card 2	13	Load side A		Clr 2nd Read	
	14	Load side B		2nd Read	
	15	Initialize		Clr A	A
	16	Overpressure	Pressure Ratio (P/P_o)	RUN	R - m
	17	Pulse Length		RUN	Δ_t - sec
	18	Repeat 16, 17 for futher (P/P_o).			

The following can serve as a test case (M107)

Step	Enter	Display
4	66.8 kg	33.4
5	914.4 m/sec	2.79×10^{7} j
6	25.93kg	25.93
7	3.173×10^{6} j/kg	5.435×10^{7} j
8	3.13×10^{3}	193.42
9	8.94 m	8.94
10	.175	51.1
11	3.66×10^{-3} m	25.
12	1.58×10^{3} kg/m^{3}	.7057
13-15		3.076×10^{-2}
16	1.2	6.044 m
17		5.12×10^{-3} sec
18 etc.		

The following is a listing of the program.

MUZZLE BLAST ANALYSIS - CARD 1A

LOC	CODE	KEY	COMMENTS
000	46	LBL*	
	11	A	
	81	HLT	(I) Proj Mass (kg)
	55	÷	
	02	2	
005	65	X	
	81	HLT	(I) Proj Vel (m/sec)
	40	X^2*	
	95	=	
	42	STO	
010	00	0	
	00	0	E_{proj}-j
	81	HLT	(I) Prop Mass (kg)
	42	STO	
	00	0	
015	01	1	M_{prop}-kg
	65	X	
	81	HLT	(I) Specific Energy (j/kg)
	95	=	
	42	STO	
020	00	0	
	02	2	E_{prop}-j
	75	-	
	43	RCL	
	00	0	
025	00	0	
	95	=	
	42	STO	
	00	0	
	03	3	E_{avail}-j
030	81	HLT	$\frac{\Delta P}{P_a}$ cham
	42	STO	
	00	0	
	04	4	$\frac{\Delta P}{P_a}$ cham
	23	LNX	
035	65	X	
	93	·	
	09	9	
	02	2	
	75	-	
040	02	2	
	93	·	
	01	1	
	04	4	
	95	=	
045	22	INV	
	23	LNX	
	42	STO	
	00	0	
	05	5	$\frac{\Delta P}{P_a}$ choke
050	81	HLT	Barrel Length-m
	55	÷	
	81	HLT	Barrel Dia-m
	42	STO	
	00	0	
055	06	6	D_{gun}-m
	95	=	
	42	STO	
	00	0	
	07	7	(L/D) Gun
060	81	HLT	
	55	÷	
	43	RCL	
	00	0	
	06	6	
065	95	=	
	42	STO	
	00	0	
	08	8	h
	45	Y^X	
070	93	·	
	01	1	
	95	=	
	20	$1/X^X$	
	65	X	
075	01	1	
	05	5	
	95	=	
	42	STO	
	00	0	
080	09	9	
	75	-	
	43	RCL	

MUZZLE BLAST ANALYSIS - CARD 1A (Cont)

LOC	CODE	KEY	COMMENTS
080	00	0	
	07	7	
085	95	=	
	80	If Pos*	
	12	B	(L/D)ch>(L/D)G
	65	X	
	01	1	
090	93	.	
	09	9	
	65	X	
	43	RCL	
	00	0	
095	08	8	
	95	=	
	85	+	
	43	RCL	
	00	0	
100	05	5	
	23	LNX	
	95	=	
	22	INV	
	23	LNX	
105	20	1/X*	
	65	X	
	43	RCL	
	00	0	
	04	4	
110	95	=	
	42	STO	

REGISTERS	
00	E_{proj}-j
01	M_{prop}-kg
02	E_{prop}-j
03	E_{avail}-j
04	$\frac{\Delta P}{P_a}$ cham
05	$(\Delta P/p_a)$ choke
06	D_{barrel}
07	$(L/D)_{Gun}$
08	h
09	(L/D) choke
10	(reduction in E_{avail})
11	Y_o - j
12	M' - M^3
13	(1/3)
14	R_o - m
15	Z_o - m
16	Z_t - m

MUZZLE BLAST ANALYSIS - CARD 1B

LOC	CODE	KEY	COMMENTS
112	01	1	
	00	0	Reduction in E_{avail}
	65	X	
	06	6	
	95	=	
117	20	1/X*	
	65	X	
	43	RCL	
	00	0	
	03	3	
122	95	=	
	42	STO	
	01	1	
	01	1	Y_o - j
	08	8	
127	93	.	
	02	2	
	52	EE	
	94	+/-	
	03	3	
132	65	X	
	43	RCL	
	00	0	
	01	1	
	95	=	
137	42	STO	
	01	1	
	02	2	M' - M^3
	02	2	
	05	5	
142	65	X	
	81	HLT	(I) Specific Grav - kg/m^3
	95	=	
	20	1/X*	
	65	X	
147	43	RCL	
	00	0	
	01	1	
	95	=	
	45	Y^X	
152	53	(	
	01	1	
	55	÷	
	03	3	

LOC	CODE	KEY	COMMENTS
152	54	)	
157	42	STO	
	01	1	
	03	3	(1/3)
	95	=	
	42	STO	
162	01	1	
	04	4	R_o - m
	45	Y^X	
	03	3	
	85	+	
167	43	RCL	
	01	1	
	02	2	
	95	=	
	45	Y^X	
172	43	RCL	
	01	1	
	03	3	
	95	=	
	42	STO	
177	01	1	
	05	5	Z_o - m
	45	Y^X	
	03	3	
	95	=	
182	20	1/X*	
	65	X	
	43	RCL	
	01	1	
	01	1	
187	95	=	
	45	Y^X	
	93	.	
	03	3	
	00	0	
192	07	7	
	07	7	
	65	X	
	01	1	
	93	.	
197	07	7	
	08	8	
	52	EE	
	94	+1-	

MUZZLE BLAST ANALYSIS - CARD 1B (Cont)

LOC	CODE	KEY	COMMENTS
	02	2	
202	65	X	
	43	RCL	
	01	1	
	05	5	
	95	=	
207	42	STO	
	01	1	
	06	6	Z_t - m
	81	HLT	
	46	LBL*	
212	12	B	
	00	0	
	20	1/X*	
	81	HLT	

MUZZLE BLAST ANALYSIS - CARD 2A

LOC	CODE	KEY	COMMENTS
000	46	LBL*	
	11	A	
	43	RCL	
	01	1	
	06	6	
005	45	Y^X	
	03	3	
	75	-	
	43	RCL	
	01	1	
010	02	2	
	95	=	
	45	Y^X	
	43	RCL	
	01	1	
015	03	3	
	95	=	
	42	STO	
	01	1	
	07	7	R_t - m
020	01	1	
	93	.	
	04	4	
	20	1/X*	
	42	STO	
025	00	0	
03	03	3	$1/\gamma$
	43	RCL	
	01	1	
	06	6	
030	45	Y^X	
	03	3	
	93	.	
	02	2	
	05	5	
035	65	X	
	09	9	
	93	.	
	05	5	
	05	5	
040	52	EE	
	94	+/-	
	02	2	
	95	=	
	42	STO	

LOC	CODE	KEY	COMMENTS
045	00	0	
	00	0	$A=Q_t Z_t q$
	46	LBL*	
	12	B	
	81	HLT	(I) P/P_o
050	42	STO	
	01	1	
	08	8	
	65	X	
	06	6	
055	85	+	
	01	1	
	95	=	
	55	÷	
	53	(	
060	43	RCL	
	01	1	
	08	8	
	85	+	
	06	6	
065	54	)	
	95	=	
	42	STO	
	00	0	
	01	1	D
070	75	-	
	01	1	
	95	=	
	55	÷	
	43	RCL	
075	00	0	
	01	1	
	95	=	
	42	STO	
	00	0	
080	02	2	(D-1)/D
	43	RCL	
	00	0	
	01	1	
	20	1/X*	
085	65	X	
	43	RCL	
	01	1	
	08	8	
	45	Y^X	

MUZZLE BLAST ANALYSIS - CARD 2A (Cont)

LOC	CODE	KEY	COMMENTS
090	43	RCL	
	00	0	
	03	3	
	75	-	
	01	1	
095	95	=	
	65	X	
	02	2	
	93	.	
	05	5	
100	95	=	
	42	STO	
	00	0	
	04	4	Q
	20	1/X*	
105	65	X	
	43	RCL	
	00	0	
	00	0	
	95	=	
110	45	Y^X	
	93	.	

REGISTERS	
00	A
01	D
02	(D-1)/D
03	$1/\gamma$
04	Q
05	
06	
07	
08	
09	
10	
11	
12	M'
13	(1/3)
14	R_o
15	Z_o
16	Z_t
17	R_t
18	P/P_a
19	Z

MUZZLE BLAST ANALYSIS - CARD 2B

LOC	CODE	KEY	COMMENTS
112	03	3	
	01	1	
	95	=	
	42	STO	
	01	1	
117	09	9	
	45	Y^x	
	03	3	
	75	-	
	43	RCL	
122	01	1	
	02	2	
	95	=	
	45	Y^x	
	43	RCL	
127	01	1	
	03	3	
	95	=	
	65	X	
	01	1	
132	93	.	
	06	6	
	02	2	
	04	4	
	95	=	Disp R-M
137	81	HLT	
	53	(	
	43	RCL	
	01	1	
	08	8	
142	75	-	
	01	1	
	54	)	
	65	X	
	43	RCL	
147	00	0	
	02	2	
	95	=	
	30	$\sqrt{\ }$*	
	65	X	
152	02	2	
	08	8	
	00	0	
	93	.	
	95	=	

LOC	CODE	KEY	COMMENTS
157	42	STO	
	00	0	
	05	5	u - m/sec
	43	RCL	
	01	1	
162	09	9	
	45	Y^x	
	53	(	
	93	.	
	02	2	
167	05	5	
	94	+/-	
	54	)	
	65	X	
	43	RCL	
172	00	0	
	00	0	
	65	X	
	43	RCL	
	00	0	
177	02	2	
	65	X	
	05	5	
	55	÷	
	43	RCL	
182	01	1	
	08	8	
	95	=	
	45	Y^x	
	43	RCL	
187	01	1	
	03	3	
	95	=	
	55	÷	
	43	RCL	
192	00	0	
	05	5	
	95	=	
	41	GTO	
	12	B	Display Δt at B

App-2. Computer Code for the Theoretical Predictions.

The theory discussed in this report was programmed in BASIC, a listing of which follows. Execution of the program produces output as illustrated in Table App - 2. The initial section requests the input quantities in the units shown. The subsequent quantities are calculated and interpreted as follows:

TOTAL ENERGY IN PROPELLANT	Total energy available
KINETIC ENERGY IN PROJECTILE	Projectile KE at the nominal muzzle velocity
MAXIMUM AVAILABLE ENERGY	$\varepsilon_t - (\varepsilon_{KE})$ proj
OVERPRESSURE RATIO (CHOKE)	Results of Bernoulli expansion
OVERPRESSURE RATIO (MUZZLE)	Includes energy impedance from rough wall
YIELD	Yield of spherical explosion
SPHERICAL RADIUS	Radius of sph. explosion
TRANSITION RADIUS (R_t)	Radius separating strong and weak shock regimes
TRANSITION VELOCITY (U_t)	Material speed at R_t

The remaining tabulation gives the range, predicted overpressure ratio, pulse length and comparisons between the predicted results and the noise level restrictions specified by the safety regulations[21]. The last two columns are interpreted as the number of shots per day which can be tolerated with single or double ear protection.

---

[21] *"Military Standard - Noise Limits for Army Material," MIL - STD - 1474A(MI, 3 Mar., 1975.*

Table App-2. Muzzle Blast Overpressure and Pulse Length

PROJECTILE	MASS (KG)	? 66.8
	VELOCITY (M/SEC)	? 914.4
PROPELLANT	MASS (KG)	? 25.93
	SPECIFIC GRAVITY (KG/M^3)	? 1.58E3
	SPECIFIC ENERGY (J/KG)	? 3.173E6
CHAMBER PRESSURE RATIO (P/PO)		? 3.13E3
BARREL	LENGTH (M)	? 8.94
	DIAMETER (M)	? .175
	GROOVE HEIGHT (M)	? 3.66E-3

ENERGY CALCULATIONS

TOTAL ENERGY IN PROPELLANT	8.22759E+7 JOULES
KINETIC ENERGY IN PROJECTILE	2.79263E+7 JOULES
MAXIMUM AVAILABLE ENERGY	5.43496E+7 JOULES

INTERIOR LOSSES

OVERPRESSURE RATIO AT 3.86443 M IS	195.476 (CHOKE)
OVERPRESSURE AT 8.94 M IS	62.7723 (MUZZLE)

EQUIVALENT EXPLOSION PARAMETERS

YIELD	181722 JOULES
SPHERICAL RADIUS	8.67565E-2 M

MUZZLE BLAST CALCULATIONS

TRANSITION RADIUS (RT)	SPHERICAL	.543517 M
	CYLINDRICAL	.882521 M
TRANSITION VELOCITY (UT)		172.67 M/SEC

Table App-2. Muzzle Blast Overpressure and Pulse Length (Cont)

RADIUS (M)	OVERPRESSURE (P-PO)/PO	PULSE LENGTH T/(RT/UT)	#ROUNDS W/PROTECTION SINGLE	DOUBLE
2	.792133	.410223	NONE	NONE
4	.328743	.736885	5	100
6	.201607	1.00585	5	100
8	.143676	1.24237	100	1000
10	.112007	1.44735	100	1000
12	9.17494E-2	1.63398	100	1000
14	7.81999E-2	1.7987	100	1000
16	6.92267E-2	1.93242	1000	>1000
18	6.21047E-2	2.05978	1000	>1000
20	5.73473E-2	2.15503	1000	>1000

```
100   FOR N=1 TO 5 STEP 1
110   PRINT
120   NEXT N
140   PRINT "MUZZLE BLAST OVERPRESSURE AND PULSE LENGTH"
150   PRINT "----------------------------------------"
160   PRINT
170   PRINT
200   REM . . . . INPUT SECTION . . . .
201   REM . . VARIABLE DEFINITIONS ARE AS FOLLOWS:
202   REM . . PROJECTILE:  V0 - VELOCITY (M/SEC),   W0 - MASS (KG)
203   REM . . PROPELLANT:  W1 - MASS (KG), X1 - SP. GRAVITY (KG/M^3)
204   REM . .              X2 - SPECIFIC ENERGY (J/KG)
205   REM . . PRESSURE:    P - CHAMBER PRESSURE RATIO (P/PA)
206   REM . . BARREL:      L0 - Length (M),   D0 - Diameter (M),
207   REM . .              L1 - GROOVE HEIGHT (RIFLING) (M)
210   PRINT "PROJECTILE", "MASS (KG)",,
220   INPUT W0
225   PRINT
230   PRINT , "VELOCITY (M/SEC)",
240   INPUT V0
245   PRINT
246   PRINT
250   PRINT "PROPELLANT","MASS (KG)",,
260   INPUT W1
265   PRINT
270   PRINT ,"SPECIFIC GRAVITY (KG/M^3)",
280   INPUT X1
285   PRINT
290   PRINT ,"SPECIFIC ENERGY (J/KG)",
300   INPUT X2
305   PRINT
306   PRINT
310   PRINT "CHAMBER PRESSURE RATIO (P/PA)",,
320   INPUT P0
325   PRINT
326   PRINT
330   PRINT "BARREL","LENGTH (M)",,
340   INPUT L0
345   PRINT
350   PRINT ,"DIAMETER (M)",,
360   INPUT D0
365   PRINT
370   PRINT ,"GROOVE HEIGHT (M)",
380   INPUT L1
390   PRINT
395   PRINT
400   REM . . END INPUT DATA
```

```
1000  REM . .
1010  REM . . BEGIN ENERGY CALCULATIONS
1011  REM . . E(PROP) = E2, E(PROJ) = E1, E(AVAIL) = E0
1020  LET E2=X2*W1
1030  LET E1=.5*W0*V0^2
1040  LET E0=E2-E1
1050  PRINT
1060  PRINT ,"   ENERGY CALCULATIONS"
1070  PRINT
1080  PRINT "TOTAL ENERGY IN PROPELLANT",,E2;"JOULES"
1090  PRINT "KINETIC ENERGY IN PROJECTILE",,E1;"JOULES"
1100  PRINT " MAXIMUM AVAILABLE ENERGY",,E0;" JOULES"
1110  LET P0=P0-1
2000  PRINT
2001  PRINT ,"   INTERIOR LOSSES"
2002  PRINT
2010  REM . . ROUGHNESS FACTOR = H, OVERPRESSURE RATIO AT CHOKE = X
2020  REM . . O´PRESSURE RATIO AT MUZZLE AND INITIAL YIELD = Y0
2021  REM . . CHOKE LENGTH = L2
2030  LET . . LET H=L1/D0
2040  LET L2=0
2050  LET X=P0
2060  REM . . IF CHOKE L/D > GUN L/D ASSUME NO CHOKE LOSSES
2065  IF H= 0 GOTO 2180
2070  IF 15/H^.1>(L0/D0) GOTO  2180
2080  lET L2=15/H^.1
2090  REM . . IF P0>100 USE FITTED CURVE
2100  IF P0>100 GOTO 2160
2110  LET X=P0
2120  LET C=(1+X)*(1+4*X^2/5/(1+X)/(9+X))^5-1
2130  IF  ABS (C-P0)<.001 GOTO  2170
2140  LET X=X-(X-1)*(C-P0)/C-1.29)
2150  GOTO 2110
2160  LET X= EXP (.9211* LOG (P0)-2.138)
2170  PRINT "OVERPRESSURE RATIO AT";L2*D0;" M IS",X;"   (CHOKE)"
2180  LET Y0= EXP ((2*H*(L2-L0/D0)+1.068* LOG (X))/1.068)
2190  PRINT "OVERPRESSURE AT";L0;" M IS",,Y0;"
2200  LET F=P0/Y0
2210  REM . . REDUCTION IN E AVAILABLE
2220  LET Y0=E0/(6*F)
2230  PRINT
2231  PRINT ,"     EQUIVALENT EXPLOSION PARAMETERS"
2232  PRINT
2240  PRINT "YIELD",,,Y0'"  JOULES"
2250  LET R0=(W1/(4*3.14159/3*6*X1))^(1/3)
2260  PRINT "SPHERICAL RADIUS",,R0;" M"
2270  REM . . END INTERIOR LOSS CALCULATIONS
3000  REM . .
```

```
3001  REM . . BEGIN OVERPRESSURE VS. DISTANCE CALCULATIONS
3002  REM . .
3010  REM . . ATMOSPHERIC CALCULATIONS AND DEFINITIONS
3020  REM . . PRESSURE (J/M^3) = P5, DENSITY (KG/M^3) = D5
3030  LET P5=101325
3040  LET D5=1.29
3050  REM . . EXPONENTS Q1&Q2, M IN MEZ, G=GAMMA, Q9=Q(TRAN),Z9=Z(TRAN)
3060  LET Q1=3.25
3070  LET Q2=3.25
3080  LET G=1.4
3090  LET M=.25*W1/(4/3*3.14159*6*D5)
3100  LET Z0=(R0^3+M)^(1/3)
3110  LET Q9=.0955
3120  REM . . SOLVE FOR TRANSITION RADIUS
3130  REM . . GET CORRECT DIMENSIONLESS YO
3140  LET Y0=.00001*Y0
3150  LET A=Y0/(4*3.14159*Q9*Z0^3)
3160  IF Q1=Q2 GOTO  3240
3170  LET B=(Q2-Q1)/(Q2-3)/(Q1-3)
3180  LET V=4
3190  LET T=(V^Q1)/(Q1-3)-B*V^3
3200  IF ABS (T/A-1)<.001 GOTO 3250
3210  LET V1=(A-T)/(Q1*(V^(Q1-1))/(Q1-3)-3*V^2*B)
3220  LET V=V+V1
3230  GOTO  3190
3240  LET V=(A/4)^(1/Q1)
3250  LET Z9=V*Z0
3251  LET R9=(Z9^3-M)^(1/3)
3252  LET R8=.8735*(1.5*(Q1-2)/(Q1-3))^(1/Q1)
3253  REM . . NOTE: R8 IS CYL. ADJUSTMENT ASSUMING Q1=Q2
3254  REM . . THERE IS NOT INCLUDED CALC. FOR UNEQUAL Q'S
3260  PRINT
3270  PRINT,"      MUZZLE BLAST CALCULATIONS"
3280  PRINT
3290  PRINT "TRANSITION RADIUS (RT)","SPHERICAL",R9;" M"
3291  PRINT ,,"CYLINDRICAL",R8*R9;" M"
3300  LET U9=172.67
3310  PRINT "TRANSITION VELOCITY (UT)",,U9;" M/SEC"
4000  REM . . BEGIN QZQ CALCULATIONS
4001  REM . . A = Q(T)*Z(T)^Q1, B = Q(T)*Z(T)^Q2, Q = WASTE HEAT
4002  REM . . PRINT HEADER
4003  PRINT
4004  PRINT "RADIUS", "OVERPRESSURE","PULSE LENGTH","#ROUNDS W/ PROTECTION"
        PROTECTION
4005  PRINT " (M)"," (P-P0)/P0","  T/(RT/UT)","SINGLE","DOUBLE"
4006  PRINT "------","----------","----------","---------------"
4009  LET P=2
4010  LET R=2/R8
```

```
4020  IF R>R0 GOTO  4050
4030  LET R=R+2/R8
4040  GOTO  4020
4050  LET Z=(R^3+M)^(1/3)
4060  LET Q5=Q1
4070  IF Z<Z9 GOTO 4090
4080  LET Q5=Q2
4090  LET Q=Q9*(Z9/Z)^Q5
4100  IF Q<2.718 GOTO 4156
4110  REM . . HIGH PRESSURE APPROXIMATION
4120  LET X=.5*(23- SQR (441-64*.4343* LOG (Q)))
4130  LET P=10^X+1
4140  GOTO 4220
4150  REM . . MEDIUM PRESSURE Q - NEWTON/RAPHSON ITERATION
4156  LET A1=(G+1)/(G-1)*P+1
4157  LET A2=P+(G+1)/(G-1)
4160  LET F=(A2*P^(1/G)-A1)-A1*(G-1)*Q
4170  LET F1=1/G*P^(1/G-1)*A2+P^(1/G)
4172  LET F1=F1-(G+1)/(G-1)-(G+1)*Q
4180  LET N=F/F1
4190  IF ABS (N)<.001 GOTO 4220
4200  LET P=P-N
4210  GOTO 4156
4220  REM . . PRESSURE RATIO OBTAINED, NEXT DELTA T
5000  REM . . SECTION FOR DELTA T
5010  REM . . Y = PROMPT ENERGY, Y = ADJUSTED ENERGY
5020  LET A=Q9*Z9^Q1
5030  IF Q1=Q2  GOTO  5130
5040  IF Z<Z9 GOTO 5060
5050  LET A=0
5060  LET Z5=Z9
5070  IF Z<Z9 GOTO 5090
5080  LET Z5=Z
5090  LET B2=A/(3-Q1)*(Z5^(3-Q1)-Z^(3-Q1))
5100  LET B=Q9*Z9^Q2
5110  LET Y5=4*3.14159*(B2-B/(3-Q2)*Z5^(3-Q2))
5120  GOTO 5140
5130  LET Y5=4*3.14159*A*Z^(3-Q1)/(Q1-3)
5140  LET D=((G+1)/(G-1)*P+1)/(P+(G+1)/(G-1))
5150  LET Y=Y5/(4/3*3.14159*P)/(1+G)*(D-1)/D
5160  LET U= SQR (P5/D5)* SQR ((P-1)*(D-1)/D)
5170  LET T=Y^(1/3)/U
5180  REM . . OUTPUT MUZZLE BLAST VALUES
5190  PRINT R*R8,(P-1),T/(R8*R9/U9),
6000  REM . . THIS SECTION REFLECTS THE SG'S SAFETY REQUIREMENTS
6001  REM . . O'PRESSURE AND PULSE LENGTH COMPARED TO STANDARD
6010  LET H9=-3.095* LOG (T*1000)+189.9
6020  LET H8=.4353*20* LOG ((P-1)*14.7*3.4475E+8)
```

```
6040  IF H8>H9 GOTO 6170
6060  IF H8>(H9-6.5) GOTO  6150
6070  IF H8>(H9-11.5) GOTO  6130
6080  IF H8>140 GOTO 6110
6090  PRINT ">1000",">1000"
6100  GOTO 7000
6110  PRINT " 1000",">1000"
6120  GOTO 7000
6130  PRINT "  100"," 1000"
6140  GOTO 7000
6150  PRINT "    5","  100"
6160  GOTO 7000
6170  PRINT " NONE"," NONE"
7000  LET R=R+2/R8
7010  IF R*R8>21 GOTO 9000
7020  GOTO 4050
9000  PRINT
9010  PRINT
9020  PRINT "OVERPRESSURE (DB) AT ";R*R8;" M IS";H8
9030  END
```

SYMBOL TABLE

A	Cross-sectional area of barrel
B	Ratio of mass prompt energy to that of air; MEZ(II-B.2)
D	Barrel hydraulic diameter
E	Energy
F	Gibbs free energy
H	Ratio of roughness height to tube diameter, h/D
I	Function in Equation (17)
K	Kinetic energy per unit mass, $1/2\ u^2$
L	Length (fixed) along barrel axis
M, M'	Mass, Mass function (MEZ)
N	Number of Particles (kinetic theory)
P	Absolute pressure
Pr	Pressure ratio, P/Pa
ΔPr	Overpressure ratio, (P-Pa)/Pa
Q	Waste heat
R	Distance from point of explosion to shock wave
S	Perimeter of barrel
T	Temperature
U	Interaction potential
V	Speed, volume
W	Pressure volume work, $W = \int Pdv$
X	Dimensionless distance (Z_t/Z_o)
Y	Prompt Energy
Z	Mass corrected R, MEZ

SYMBOL TABLE, L.C.

a	Speed of sound
e	Specific energy, (E/mass)
h	Height of barrel roughness
k	Boltzmann's constant
q	Exponent in QZQ hypothesis
r	Radial coordinate
t	Time
u	Material velocity behind shockwave
v	Specific volume
x	Dimensionless distance, (L/D), in gun
z	Coordinate along barrel axis

Subscripts

a	Ambient
c	Choke joint
f	Final
I	Initial, internal
K.E.	Kinetic energy
p	Peak value
T	Total
o	At charge
t	Transition

Greek

α	Proportionality constant
β	$2\gamma/(\gamma-1)$
γ	Ratio of specific heats
ε	Energy per unit volume
$\xi\ \eta$	Constants in intermediate calculations
μ	$(\gamma+1)/(\gamma-1)$
ρ	Density
θ	Angle between unit normal along barrel axis and position vector from muzzle to pressure probe.

DISTRIBUTION LIST

No. of Copies	Organization
12	Commander Defense Documentation Center ATTN: DDC-TCA Cameron Station Alexandria, VA 22314
3	Director Defense Advanced Research Projects Agency ATTN: Tech Lib NMRO PMO 1400 Wilson Boulevard Arlington, VA 22209
5	Director of Defense Research & Engineering ATTN: DD/TWP DD/S&SS DD/T&SS AD/SW Mr. J. Persh, Staff Specialist Materials and Structures WASH, DC 20301
1	Director Institute for Defense Analyses ATTN: IDA Librarian, Ruth S. Smith 400 Army-Navy Drive Arlington, VA 22202
2	Asst. to the Secretary of Defense (Atomic Energy) ATTN: Document Control Donald R. Cotter WASH, DC 20301
4	Director Defense Intelligence Agency ATTN: DT-1C/Dr. J. Vorona DI-7D/E.O. Farrell DT-2/Wpns & Sys Div Technical Library WASH, DC 20301
6	Director Defense Nuclear Agency ATTN: SPTD/Mr. J. Kelso SPSS/Dr. E. Sevin SPAS/Mr. J. Moulton STSP STVL/Dr. LaVier RATN/Cdr Alderson WASH, DC 20305
6	Director Defense Nuclear Agency ATTN: DDST/Mr. P. Hass DDST/Mr. M. Atkins STTL/Tech Lib (2 cy) STSI/Archives SPSS/LT J.R. Williams WASH, DC 20305
1	Commander Field Command, DNA ATTN: FCPR Kirtland AFB, NM 87115
1	Chief Las Vegas Liaison Office Field Command TD, DNA ATTN: Document Control P.O. Box 2702 Las Vegas, NV 89104

DISTRIBUTION LIST

No. of Copies	Organization
1	Commander Field Command, DNA Livermore Branch ATTN: FCPRL P. O. Box 808 Livermore, CA 94550
1	Director Defense Communications Agency ATTN: NMCSSC (Code 510) Washington, DC 20305
1	Director Joint Strategic Target Planning Staff JCS ATTN: Sci & Tech Info Lib Offutt AFB Omaha, NB 68113
2	Director National Security Agency ATTN: E. F. Butala, R154 P. E. Deboy, NSA 5232 Ft. George G. Meade, MD 20755
1	Commander US Army Materiel Development and Readiness Command ATTN: DRCDMA-ST 5001 Eisenhower Avenue Alexandria, VA 22333
1	Commander US Army Aviation Research and Development Command ATTN: DRSAV-E 12th and Spruce Streets St. Louis, MO 63166
1	Director US Army Air Mobility Research and Development Laboratory Ames Research Center Moffett Field, CA 94035
4	Commander US Army Electronics Command ATTN: DRSEL-RD DRSEL-TL-IR R. Freiberg J. Roma A. Sigismondi Fort Monmouth, NJ 07703
2	Commander US Army Missile Research and Development Command ATTN: DRDMI-R Technical Library Redstone Arsenal, AL 35809
1	Commander US Army Missile Research and Development Command ATTN: DRCPM-MDEI Redstone Arsenal, AL 35809
1	Commander US Army Tank Automotive Research & Development Cmd ATTN: DRDTA-RWL Warren, MI 48090
1	Commander US Army Mobility Equipment Research & Development Cmd ATTN: Tech Docu Cen, Bldg 315 DRSME-RZT Fort Belvoir, VA 22060
1	Commander US Army Armament Materiel Readiness Command ATTN: DRSAR-LEP-L, Tech Lib Rock Island, IL 61299
1	Commander US Army Armament Research and Development Command ATTN: DRDAR-LC, G.Demitrack Dover, NJ 07801

DISTRIBUTION LIST

No. of Copies	Organization
1	Commander US Army White Sands Missile Range ATTN: STEWS-TE-N/Mr. J. Gorman White Sands, NM 88002
1	Commander US Army Watervliet Arsenal Watervliet, NY 12189
5	Commander US Army Harry Diamond Labs ATTN: DRXDO-TI DRXDO-TI/012 Mr. F. N. Wimenitz Mr. Jim Gaul DRXDO-NP Mr. J. Gwaltney DRXDO-RBH Mr. P. A. Caldwell 2800 Powder Mill Road Adelphi, MD 20783
1	Commander US Army Materials and Mechanics Research Center ATTN: Tech Lib Watertown, MA 02172
1	Commander US Army Natick Research and Development Command ATTN: DRXRE, Dr. D. Sieling Natick, MA 01762
1	Commander US Army Foreign Science and Technology Center ATTN: Rsch & Data Branch Federal Office Building 220 7th Street, NE Charlottesville, VA 22901
1	Director US Army TRADOC Systems Analysis Activity ATTN: ATAA-SL, Tech Lib White Sands Missile Range NM 88002
3	Commander US Army Nuclear Agency ATTN: ATCN-W/CPT Ader CDINS-E Technical Library 7500 Backlick Rd., Bldg 2073 Springfield, VA 22150
1	Commander US Army Communications Command ATTN: Tech Library Fort Huachuca, AZ 85613
1	Interservice Nuclear Weapons School ATTN: Technical Library Kirtland AFB, NM 87115
2	HQDA (DAMA-MC; NCB Div) Washington, DC 20310
2	HQDA (DAEN-MC; DAEN-CWE) Washington, DC 20310
2	Office, Chief of Engineers Department of the Army Publications Department ATTN: DAEN-MCE-D DAEN-RDM 890 South Pickett Street Alexandria, VA 22304

DISTRIBUTION LIST

No. of Copies	Organization
3	Director US Army BMD Advanced Technology Center ATTN: CRDABH-X/J. Davidson CRDABH-S/Mr. M. Capps N.J. Hurst P.O. Box 1500, West Station Huntsville, AL 35807
1	Commander US Army Research Office PO Box 12211 Research Triangle Park, NC 27709
4	Commander US Army Engineer Waterways Experiment Station ATTN: Technical Library William Flathau John N. Strange James Ballard P.O. Box 631 Vicksburg, MS 39180
2	Director Defense Civil Preparedness Agency ATTN: Mr. George Sisson/RF-SR Technical Library Washington, DC 20301
1	Commander US Army Engineering Center ATTN: ATSEN-SY-L Fort Belvoir, VA 22060
1	Director US Army Construction Engineering Research Laboratory ATTN: CERL-SL P.O. Box 4005 Champaign, IL 61820
1	Division Engineer US Army Engineering Division ATTN: Docu Cen Ohio River P.O. Box 1159 Cincinnati, OH 42501
1	Division Engineer US Army Engineering Division ATTN: Mr. M. Dembo Huntsville Box 1600 Huntsville, AL 35804
5	Chief of Naval Research ATTN: Code 464/Jacob L. Warner Code 464/Thomas P. Quinn N. Perrone (2 cy) Technical Library Department of the Navy WASH, DC 20360
2	Chief of Naval Operations ATTN: OP-03EG OP-985F Department of the Navy WASH, DC 20350
1	Chief of Naval Material ATTN: MAT 0323 Department of the Navy Arlington, VA 22217
1	Director Strategic Systems Project Ofc ATTN: NSP-43, Tech Lib Department of the Navy WASH, DC 20360
1	Commander Naval Electronic Systems Cmd ATTN: PME 117-21A WASH, DC 20360

DISTRIBUTION LIST

No. of Copies	Organization
2	Commander Naval Sea Systems Command ATTN: ORD-91313 Library Code 03511 Department of the Navy Washington, DC 20362
3	Commander US Naval Facilities Engineering Command ATTN: Code 03A Code 04B Technical Library Washington, DC 20360
2	Commander Naval Ship Engineering Center ATTN: Technical Library NSEC 6105G Hyattsville, MD 20782
1	Commander David W. Taylor Naval Ship Research & Development Ctr ATTN: L42-3 Library Bethesda, MD 20084
3	Commander US Naval Surface Weapons Ctr ATTN: Code 1224/Navy Nuclear Programs Office Code CR14/Tech Lib Francis B. Porzel Silver Spring, MD 20910
1	Commander US Naval Surface Weapons Ctr ATTN: Technical Library Dahlgren, VA 22448
2	Commander US Naval Ship Research and Development Center Facility Underwater Explosions Research Division ATTN: Code 17, W.W. Murray Technical Library Portsmouth, VA 23709
1	Commander US Naval Weapons Evaluation Facility Kirtland AFB Albuquerque, NM 87117
2	Commander and Director US Naval Civil Engineer Laboratory ATTN: Code L31/Mr. Shaw Mr. R. Siebold Port Hueneme, CA 93041
3	Officer-in-Charge Civil Engineering Laboratory Naval Constr Btn Center ATTN: Stan Takahashi R. J. Odello Technical Library Port Hueneme, CA 93041
2	Commander US Naval Research Laboratory ATTN: Code 2027, Tech Lib Code 8440, F. Rosenthal Washington, DC 20375
1	Superintendent US Naval Postgraduate School ATTN: Code 2124, Tech Rpts Lib Monterey, CA 93940

DISTRIBUTION LIST

No. of Copies	Organization
1	HQ USAF (SAFRD) WASH, DC 20330
1	HQ USAF (INATA) WASH, DC 20330
1	HQ USAF (PRF) WASH, DC 20330
2	AFSC (DLCAW; Tech Lib) Andrews AFB WASH, DC 20331
2	AFATL (ATRD/R. Brandt) Eglin AFB, FL 32542
1	RADC (FMTLD/Docu Lib) Griffiss AFB, NY 13340
1	AFSWC (SWTSX) Kirtland AFB, NM 87117
1	AFWL (SUL) Kirtland AFB, NM 87117
3	AFWL (Robert Port; DEV Jimmie L. Bratton; DEV M.A. Plamondon) Kirtland AFB, NM 87117
1	Commander-in-Chief Strategic Air Command ATTN: NRI-STINFO Lib Offut AFB, NB 68113
1	AFFDL (FDTR) (Dr. F.J. Janik, Jr. Wright-Patterson AFB, OH 45433
1	AFML (MAMD/Dr. T. Nicholas) Wright-Patterson AFB OH 45433
1	FTD (TDPTN) Wright-Patterson AFB OH 45433

No. of Copies	Organization
1	AFIT (Lib Bldg. 640, Area B) Wright-Patterson AFB, OH 45433
1	Director US Bureau of Mines ATTN: Technical Library Denver Federal Center Denver, CO 80225
1	Director US Bureau of Mines Twin Cities Research Center ATTN: Technical Library P.O. Box 1660 Minneapolis, NM 55111
1	US Energy Research and Development Administration Division of Headquarters Svcs ATTN: Doc Control for Classified Tech Lib Library Branch G-043 Washington, DC 20545
1	US Energy Research and Development Administration Albuquerque Operations Office ATTN: Doc Control for Tech Lib P.O. Box 5400 Albuquerque, NM 87115
1	US Energy Research and Development Administration Nevada Operations Office ATTN: Doc Control for Tech Lib P.O. Box 14100 Las Vegas, NV 89114
2	Director Lawrence Livermore Laboratory ATTN: Larry W. Woodruff, L-125 Technical Information Div P.O. Box 808 Livermore, CA 94550

DISTRIBUTION LIST

No. of Copies	Organization
1	Director Los Alamos Scientific Lab ATTN: Doc Control for Rpt Lib P.O. Box 1663 Los Alamos, NM 87544
1	Director NASA Scientific and Tech Info Facility ATTN: SAK/DL P.O. Box 8757 Baltimore/Washington International Airport, MD 21240
1	National Academy of Sciences ATTN: Mr. D.G. Groves 2101 Constitution Avenue,NW WASH, DC 20418
1	Agbabian Associates ATTN: M. Agbabian 250 North Nash Street El Segundo, CA 90245
2	Applied Theory, Inc. ATTN: John G. Trulio 1010 Westwood Blvd. Los Angeles, CA 90024
1	AVCO Government Products Group ATTN: Res Lib A830, Rm 7201 201 Lowell Street Wilmington, MA 01887
1	AVCO Structures & Mechanics Dept. ATTN: Dr. William Broding Mr. J. Gilmore Wilmington, MA 01887
1	The BDM Corporation ATTN: Technical Library 1920 Aline Avenue Vienna, VA 22180
1	Bell Telephone Labs, Inc. ATTN: Tech Rpt Ctr Mountain Avenue Murray Hill, NJ 07971
1	The Boeing Company ATTN: Aerospace Library P.O. Box 3707 Seattle, WA 98124
2	California Research and Technology, Inc. ATTN: Ken Kreyenhagen Technical Library 6269 Variel Avenue Woodland Hills, CA 91364
1	Calspan Corporation ATTN: Technical Library P.O. Box 235 Buffalo, NY 14221
1	Civil/Nuclear Systems Corp ATTN: Robert Crawford 1200 University N.E. Albuquerque, NM 87102
1	EG&G, Incorporated Albuquerque Division ATTN: Technical Library P.O. Box 10218 Albuquerque, NM 87114
1	General American Trans Corporation General American Res Div ATTN: G.L. Neidhardt 7449 N. Matchez Avenue Niles, IL 60648
1	General Electric Company-TEMPO ATTN: DASIAC P.O. Drawer QQ Santa Barbara, CA 93102

DISTRIBUTION LIST

No. of Copies	Organization
1	President General Research Corporation ATTN: Library McLean, VA 22101
1	Honeywell, Inc. Govt & Aero Products Div 600 Second Street, NE Hopkins, MN 55343
1	J.G. Engineering Research Associates 3831 Menlo Drive Baltimore, MD 21215
1	J.L. Merritt Consulting & Special Engineering Services, Inc. ATTN: Technical Library P. O. Box 1206 Redlands, CA 92373
2	Kaman AviDyne ATTN: Dr. N. P. Hobbs Mr. S. Cricione 83 Second Avenue Northwest Industrial Park Burlington, MA 01803
2	Kaman Sciences Corporation ATTN: Library Dr. Don Sachs 1500 Garden of the Gods Road Colorado Springs, CO 80907
2	Lockheed Missiles & Space Co ATTN: T. Gerrs D/52-53 Bldg 205 Tech Info Ctr, Doc/Coll. 3251 Hanover Street Palo Alto, CA 94304
1	McDonnell Douglas Corporation ATTN: Robert W. Halprin 5301 Bolsa Avenue Huntington Beach, CA 92647
1	The Mitre Corporation ATTN: Library Rt 62 and Middlesex Turnpike P. O. Box 208 Bedford, MA 01730
2	Physics International Corp. ATTN: E. T. Moore Dennis Orphas 2700 Merced Street San Leandro, CA 94577
4	Physics International Corp. ATTN: Robert Swift Charles Godfrey Larry A. Behrmann Technical Library 2700 Merced Street San Leandro, CA 94577
5	R&D Associates ATTN: Dr. H. L. Brode Dr. Albert L. Latter Bruce Hartenbaum William B. Wright Henry Cooper P. O. Box 9695 Marina del Rey, CA 90291
4	R&D Associates ATTN: Jerry Carpenter Sheldon Schuster J.G. Lewis Technical Library P. O. Box 9695 Marina del Rey, CA 90291
1	Sandia Laboratories ATTN: Doc Control for 3141 Sandia Report Coll. Albuquerque, NM 87115

DISTRIBUTION LIST

No. of Copies	Organization
2	Sandia Laboratories Livermore Laboratory ATTN: Doc Control for Tech Lib Doc Control for L.Hill P.O. Box 969 Livermore, CA 94550
1	Science Applications, Inc. ATTN: R.A. Shunk P.O. Box 3507 Albuquerque, NM 87110
3	Science Applications, Inc. ATTN: R. Seebaugh William M. Layson John Mansfield 1651 Old Meadow Road McLean, VA 22101
2	Science Applications, Inc. ATTN: David Bernstein D.E. Maxwell 8201 Capwell Drive Oakland, CA 94621
2	Science Applications, Inc. ATTN: Technical Library Michael McKay P.O. Box 2351 LaJolla, CA 92038
1	Shock Hydrodynamics, Inc. A Division of Whittaker Corp ATTN: L. Zernow 4710-16 Vineland Avenue North Hollywood, CA 91602
5	Systems, Science & Software ATTN: Robert T. Allen Donald R. Grine Ted Cherry Thomas D. Riney Technical Library P.O. Box 1620 LaJolla, CA 92037
2	Terra Tek, Inc. ATTN: Sidney Green Technical Library 420 Wakara Way Salt Lake City, UT 84108
2	Tetra Tech, Inc. ATTN: Li-San Hwang Technical Library 630 North Rosemead Blvd. Pasadena, CA 91107
7	TRW Systems Group ATTN: Paul Lieberman Benjamin Sussholtz Norm Lipner William Rowan Jack Farrell Pravin Bhutta Tech Info Ctr/S-1930 One Space Park Redondo Beach, CA 90278
2	TRW Systems Group ATTN: Mr. F.A. Pieper Greg Hulcher San Bernardino Operations P.O. Box 1310 San Bernardino, CA 92402
2	Union Carbide Corporation Holifield National Laboratory ATTN: Doc Control for Tech Lib Civil Defense Res Proj P.O. Box X Oak Ridge, TN 37830
1	Universal Analytics, Inc. ATTN: E.I. Field 7740 W. Manchester Blvd. Playa Del Rey, CA 90291

DISTRIBUTION LIST

No. of Copies	Organization
1	URS Research Company ATTN: Technical Library 155 Bovet Road San Mateo, CA 94402
1	Weidlinger Assoc. Consulting Engineers ATTN: J. Isenbert 2710 San Hill Road Suite 230 Menlo Park, CA 99025
1	Westinghouse Electric Co. Marine Division ATTN: W.A. Volz Hendy Avenue Sunnyvale, CA 94008
1	Battelle Columbus Laboratories ATTN: Technical Library 505 King Avenue Columbus, OH 43201
4	Denver Research Institute University of Denver ATTN: Mr. J. Wisotski Fred P. Vanditti Ron W. Buchanon Technical Library P.O. Box 10127 Denver, CO 80210
3	IIT Research Institute ATTN: Milton R. Johnson R.E. Welch Technical Library 10 West 35th Street Chicago, IL 60616
2	Lovelace Foundation for Medical Education ATTN: Asst Dir of Research/ Robert K. Jones Technical Library 5200 Gibson Blvd, SE Albuquerque, NM 87108
1	Massachusetts Institute of Technology Aeroelastic and Structures Research Laboratory ATTN: Dr. E.A. Witmer Cambridge, MA 02139
2	Southwest Research Institute ATTN: Dr. W.E. Baker A.B. Wenzel 8500 Culebra Road San Antonio, TX 78206
4	Stanford Research Institute ATTN: Dr. G.R. Abrahamson Carl Peterson Burt R. Gasten SRI Library, Rm G021 333 Ravenswood Avenue Menlo Park, CA 94025
1	University of California Berkeley Campus, Rm 8 ATTN: G.Sackman 2543 Channing Way Berkeley, CA 94720
1	University of Dayton ATTN: Hallock F. Swift 300 College Park Avenue Dayton, OH 45409
1	University of Florida Department Engineering Science ATTN: Dr. D. R. Keefer Gainesville, FL 32601
1	University of Illinois Consulting Engineering Services ATTN: Nathan M. Newmark 1114 Civil Engineering Bldg. Urbana, IL 61801

DISTRIBUTION LIST

No. of Copies	Organization
2	The University of New Mexico The Eric H. Wang Civil Engineering Rsch Facility ATTN: Larry Bickle Neal Baum University Station, Box 188 Albuquerque, NM 87131
2	Washington State University Administration Office ATTN: Arthur Miles Hohorf George Duval Pullman, WA 99163

Aberdeen Proving Ground

Marine Corps Ln Ofc
Dir, USAMSAA
ATTN: Dr. J. Sperrazza
Mr. R. Norman, GWD
Dr. Rivello
R. Bailey